

AD-A168 404

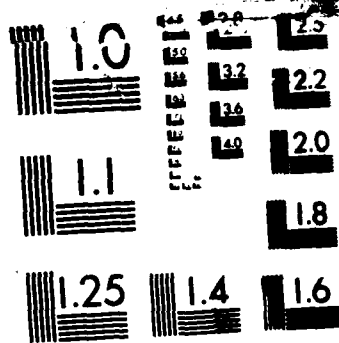
STATE-SPACE ANALYSIS OF THE TRIDENT II MARK 6 BYRO(U)
NAVAL POSTGRADUATE SCHOOL MONTEREY CA D L KRUEGER
MAR 86

1/1

UNCLASSIFIED

F/G 17/7

NL



MICROCOPY RESOLUTION TEST CHART
 NATIONAL BUREAU OF STANDARDS-1963-A

2

AD-A168 404

NAVAL POSTGRADUATE SCHOOL

Monterey, California



DTIC
SELECTE
JUN 09 1986
S D

THESIS

STATE-SPACE ANALYSIS OF
THE TRIDENT II MARK 6 GYRO

by
David L. Krueger
March 1986

Thesis Advisor: F. L. Collins

Approved for public release; distribution is unlimited.

DTIC FILE COPY

SECURITY CLASSIFICATION OF THIS PAGE

REPORT DOCUMENTATION PAGE

1a REPORT SECURITY CLASSIFICATION UNCLASSIFIED			1b. RESTRICTIVE MARKINGS	
2a SECURITY CLASSIFICATION AUTHORITY			3 DISTRIBUTION/AVAILABILITY OF REPORT Approved for public release; distribution is unlimited.	
2b DECLASSIFICATION/DOWNGRADING SCHEDULE				
4 PERFORMING ORGANIZATION REPORT NUMBER(S)			5 MONITORING ORGANIZATION REPORT NUMBER(S)	
6a NAME OF PERFORMING ORGANIZATION Naval Postgraduate School		6b OFFICE SYMBOL (if applicable) 67	7a NAME OF MONITORING ORGANIZATION Naval Postgraduate School	
6c ADDRESS (City, State, and ZIP Code) Monterey, California 93943-5000			7b ADDRESS (City, State, and ZIP Code) Monterey, California 93943-5000	
8a NAME OF FUNDING/SPONSORING ORGANIZATION		8b OFFICE SYMBOL (if applicable)	9 PROCUREMENT INSTRUMENT IDENTIFICATION NUMBER	
8c ADDRESS (City, State, and ZIP Code)			10 SOURCE OF FUNDING NUMBERS	
			PROGRAM ELEMENT NO	PROJECT NO
11 TITLE (Include Security Classification) STATE-SPACE ANALYSIS OF THE TRIDENT II MARK 6 GYRO				
12 PERSONAL AUTHOR(S) Krueger, David L.				
13a TYPE OF REPORT Master's Thesis		13b TIME COVERED FROM TO		14 DATE OF REPORT (Year, Month, Day) 1986 March
15 PAGE COUNT 70				
16 SUPPLEMENTARY NOTATION				
17 COSATI CODES			18 SUBJECT TERMS (Continue on reverse if necessary and identify by block number) Gyro; Mark 6 Gyro; Trident II missile system; optimal control; region controller	
FIELD	GROUP	SUB-GROUP		
19 ABSTRACT (Continue on reverse if necessary and identify by block number) This thesis conducts a state-space analysis of the Mark 6 gyro used in the Trident II missile system. Optimal control techniques, utilizing a region controller, have been employed in designing a gyro controller. The response of the system to missile motion is examined and compared to the system response using the current control laws. It is shown that an optimal region controller reduces the gyro error in the system while effectively avoiding gimbal lock, a situation which exists when gyro orientation prevents missile motion from being isolated in an orthogonal three axis coordinate system. Recommendations for the application of additional modern control techniques are included.				
20 DISTRIBUTION/AVAILABILITY OF ABSTRACT <input checked="" type="checkbox"/> UNCLASSIFIED/UNLIMITED <input type="checkbox"/> SAME AS RPT <input type="checkbox"/> DTIC USERS			21 ABSTRACT SECURITY CLASSIFICATION UNCLASSIFIED	
22a NAME OF RESPONSIBLE INDIVIDUAL Daniel J. Collins			22b TELEPHONE (Include Area Code) 408-646-2826	22c OFFICE SYMBOL 67

Approved for public release; distribution is unlimited.

State-Space Analysis
Of
the Trident II Mark 6 Gyro

by

David L. Krueger
Lieutenant, United States Navy
B. S. , United States Naval Academy, 1979

Submitted in partial fulfillment of the
requirements for the degree of

MASTER OF SCIENCE IN AERONAUTICAL ENGINEERING

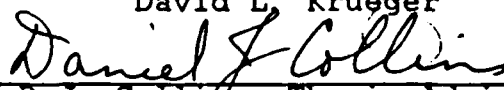
from the

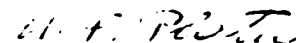
NAVAL POSTGRADUATE SCHOOL
March 1986

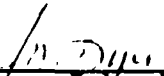
Author:


David L. Krueger

Approved by:


D. J. Collins, Thesis Advisor


M. F. Platzter, Chairman,
Department of Aeronautics


John N. Dyer,
Dean of Science and Engineering

ABSTRACT

This thesis conducts a state-space analysis of the Mark 6 gyro used in the Trident II missile system. Optimal control techniques, utilizing a region controller, have been employed in designing a gyro controller. The response of the system to missile motion is examined and compared to the system response using the current control laws. It is shown that an optimal region controller reduces the gyro error in the system while effectively avoiding gimbal lock, a situation which exists when gyro orientation prevents missile motion from being isolated in an orthogonal three axis coordinate system. Recommendations for the application of additional modern control techniques are included.

Keywords: Optimal control, Trident II, computer aided design

Accession For	
NTIS CRA&I	<input checked="" type="checkbox"/>
DTIC TAB	<input type="checkbox"/>
Unannounced	<input type="checkbox"/>
Justification	
By	
Distribution /	
Availability Codes	
Dist	Avail and/or Special
A-1	

TABLE OF CONTENTS

I.	INTRODUCTION.	8
II.	FUNCTION OF THE GYRO CONTROLLER	10
	A. THE ALL-ATTITUDE GIMBAL ASSEMBLY	10
	1. Gimbal Lock	10
	2. Missile to Stable Member Motion Coupling	10
III.	MARK 6 GYRO MODEL	13
	A. BLOCK DIAGRAM	13
	1. Plant Diagram	13
	2. Gyro Controller	17
IV.	STATE-SPACE MODEL	20
	A. BLOCK DIAGRAM	20
	1. Plant Model	20
	2. Assumptions and Simplifications	20
	3. State-Space Equations	20
V.	OPTIMIZATION TECHNIQUE	24
	A. OPTIMAL REGULATOR	24
	1. Linear Quadratic Problem	24
	2. Choice of Weighting Matrices	26
	3. Non-zero Steady State Outputs	26
	B. MARK 6 GYRO OPTIMAL CONTROLLER	27
	1. Region Controller	28
VI.	SYSTEM SIMULATION	30
	A. SIMULATION MODEL	30
	B. WEIGHTING MATRICES	30
	1. Torque Limits	30
	2. State Output Weighting Matrix R_1	30

3.	Control Input Weighting Matrix R_2	34
C.	TEST PARAMETERS	35
1.	Initial Conditions	35
2.	Missile Motion	36
D.	TEST RESULTS	36
VII.	CONCLUSIONS AND RECOMMENDATIONS	42
A.	CONCLUSIONS	42
1.	Optimal Design Techniques	42
B.	RECOMMENDATIONS	43
1.	Improving System Performance	43
APPENDIX A:	DEFINITIONS	44
APPENDIX B:	FOUR GIMBAL GYRO STATE AND ERROR EQUATION DEVELOPMENT	45
1.	FOUR GIMBAL IMU MODEL	45
1.	Assumptions and Approximations	45
2.	Definitions	45
3.	Symbols	46
4.	Transformation of missile motion to inertial member	46
APPENDIX C:	OPTIMAL CONTROL PROGRAM LISTING	51
APPENDIX D:	TABULATED DATA	66
LIST OF REFERENCES		68
INITIAL DISTRIBUTION LIST		69

LIST OF TABLES

I	STATE AND CONTROL VECTORS	22
II	OUTPUT STATE VECTOR MAXIMUM VALUES	33
III	VARIABLE DEFINITIONS	44

LIST OF FIGURES

2.1	Four Gimbal Gyro Model	11
2.2	Four Gimbal Gyro Coordinate Systems	12
3.1	Mark 6 Gyro Model (Inertial Mode)	14
3.2	Resolution of Outer and Middle Gimbal Inertias . .	15
3.3	Gimbal Lock Avoidance Switching Line	17
3.4	Mark 6 Gyro Control Law	18
4.1	State-Space Model of the Mark 6 Gyro	21
4.2	Plant and Control Matrices for State-Space Model	23
5.1	Optimal Gain Feedback Block Diagram	27
5.2	Region Controller Segments	29
5.3	Algorithm for the Mark 6 Gyro Optimal Regulator . .	29
6.1	State-Space Simulation Model of the Mark 6 Gyro . .	31
6.2	Plant Matrix for the State-Space Simulation Model	32
6.3	Control Matrix for the State Space Simulation Model	33
6.4	U and V gyro Errors for the State-Space Model . . .	37
6.5	UGSGF Errors - Draper Lab and State-Space Models	39
6.6	VGSGF Errors - Draper Lab and State-Space Models	40
6.7	Inner and Middle Gimbal Angles	41
B.1	Four Gimbal Gyro Block Diagram	50

I. INTRODUCTION

A need for accurate, self-contained navigation systems has existed since the early days of aircraft design. The most common of these systems uses accelerometers to determine body motion. The output signal is integrated once to obtain velocity and again to obtain position.

In order for the navigation system to accurately determine body motion the sensors must be mounted on a platform fixed in a known coordinate system. In ballistic missile guidance systems, gyros are used to fix a platform in inertial space. The accelerometers are mounted on this platform. The purpose of the gyro controller, then, is to generate the gyro torque motor commands necessary to maintain the stable platform fixed in inertial space.

Since 1957, the Charles Stark Draper Laboratory in Cambridge, Massachusetts has designed the gyros for the Navy's Polaris, Poseidon and Trident missiles. Because of the complex, highly non-linear nature of the control system, this design process has been a tedious, iterative affair. Using state-space representation of systems, computer-aided optimal control design techniques greatly simplify the multi-input, multi-output non-linear time varying problem. The goal of this thesis is the development of a state-space model of the Trident II gyro system, the Mark 6, and the application of modern control theory to improve system performance.

A state-space model of the system has been developed and is compared to the current gyro model. Transient response of both systems to missile motion is examined. Modern control techniques using optimal feedback gains are employed to minimize gyro errors and improve system response. The choice of optimal feedback gains is made based on a region

controller which selects the gains dependent upon the particular gimbal angles. Finally, suggestions are made for employing modern control techniques to further optimize system performance.

II. FUNCTION OF THE GYRO CONTROLLER

A. THE ALL-ATTITUDE GIMBAL ASSEMBLY

The inertial navigation system for a ballistic missile must accurately determine missile motion in three orthogonal planes. Missile motion is resolved by accelerometers mounted on a platform fixed in inertial space. A three dimensional coordinate system is initialized before missile launch, and remains fixed through out the flight. The function of the gyro controller is to keep the stable platform fixed throughout the flight.

The Mark 6 gyro consists of four concentric gimbals as shown in Figure 2.1 [Ref. 1: p. 2]. The innermost gimbal is the stable platform, housing the accelerometers. As the missile experiences pitch, roll and yaw a torque is applied to the gimbals in such a manner as to isolate the stable member from the motion.

1. Gimbal Lock

In addition to maintaining a fixed inertial reference, the gyro controller must prevent "gimbal lock". This occurs when the gimbals are co-planar and it becomes impossible to isolate missile motion on three orthogonal axes. Controlling the gyro errors is relatively straightforward, while preventing gimbal lock is more complex. Since the gimbal angles can assume any value during missile flight, the problem becomes non-linear and difficult to solve. The technique developed by Draper Laboratory for preventing gimbal lock will be employed in the design of the state-space system model. This technique is more fully described in the next chapter.

2. Missile to Stable Member Motion Coupling

The four gimbal IMU model is shown in Figure 2.2 [Ref. 2: p. 2]. Missile, or base motion occurs in the

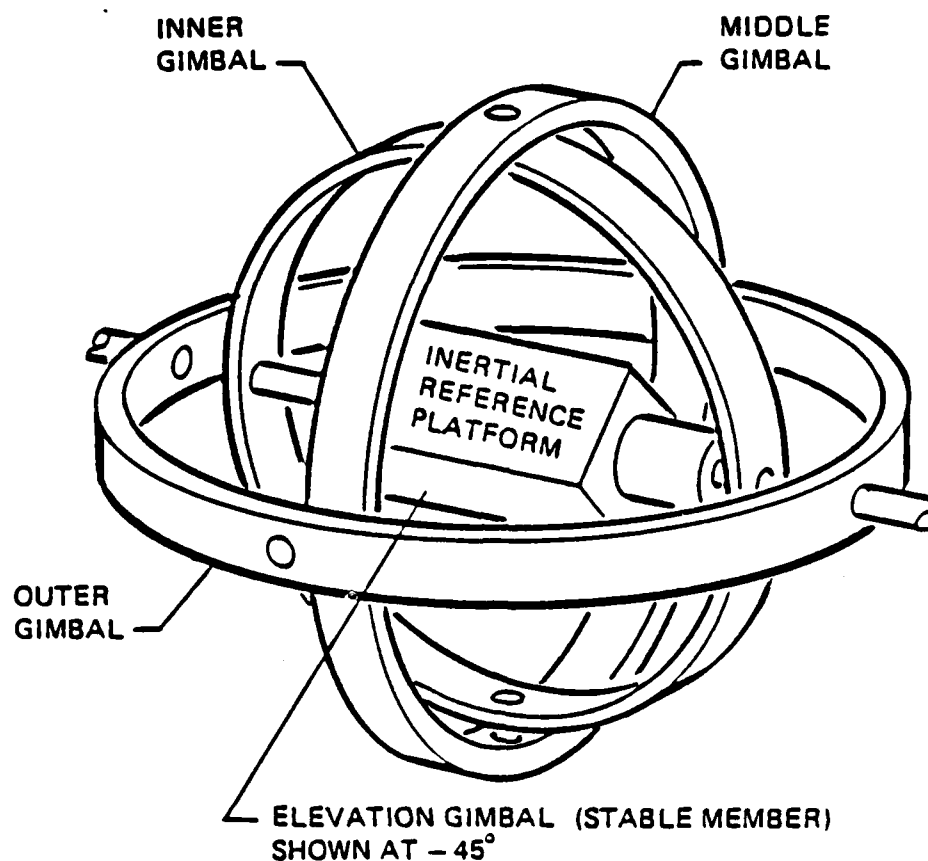


Figure 2.1 Four Gimbal Gyro Model.

i_5, j_5, k_5 coordinate system. This motion is coupled to the stable member coordinate system i_1, j_1, k_1 by the outer, middle and inner gimbals. The system accuracy is measured by the gyro error of the stable member in the i_1, j_1, k_1 space. Appendix B contains the detailed transformation of missile motion in the base frame of reference to motion in the inertial frame.

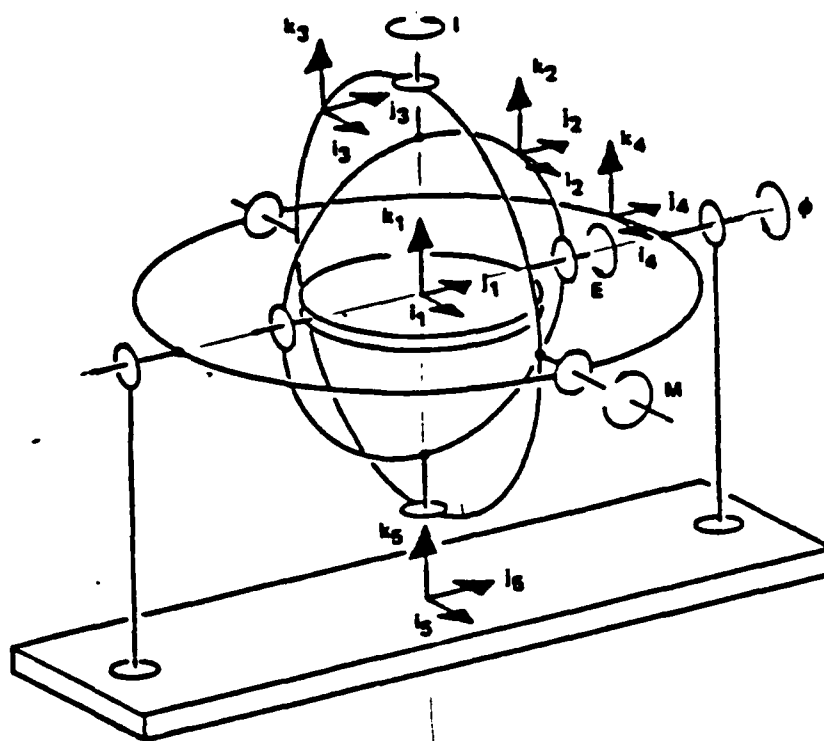


Figure 2.2 Four Gimbal Gyro Coordinate Systems.

III. MARK 6 GYRO MODEL

A. BLOCK DIAGRAM

The Mark 6 Gyro model presently being used by Draper Laboratory is shown in Figure 3.1 [Ref. 2: p. 8]. Table III in Appendix A contains a definition of abbreviations used in this thesis. The torque motor commands are the inputs to the system, with the gyro errors and gimbal angles as the output. The diagram illustrates the cross-coupling between gimbals represented by the input equations shown in Figure B.1.

1. Plant Diagram

a. Signal Conversions

Figure 3.1 contains the electrical and mechanical realizations of the Mark 6 gyro. The input signal is expressed in terms of quanta, with one quanta equal to 0.0735 volts. The torque command is expressed in ounce-inches. The gimbal angles, given in radians, are converted to quanta for input to the feedback controller.

b. RGyro

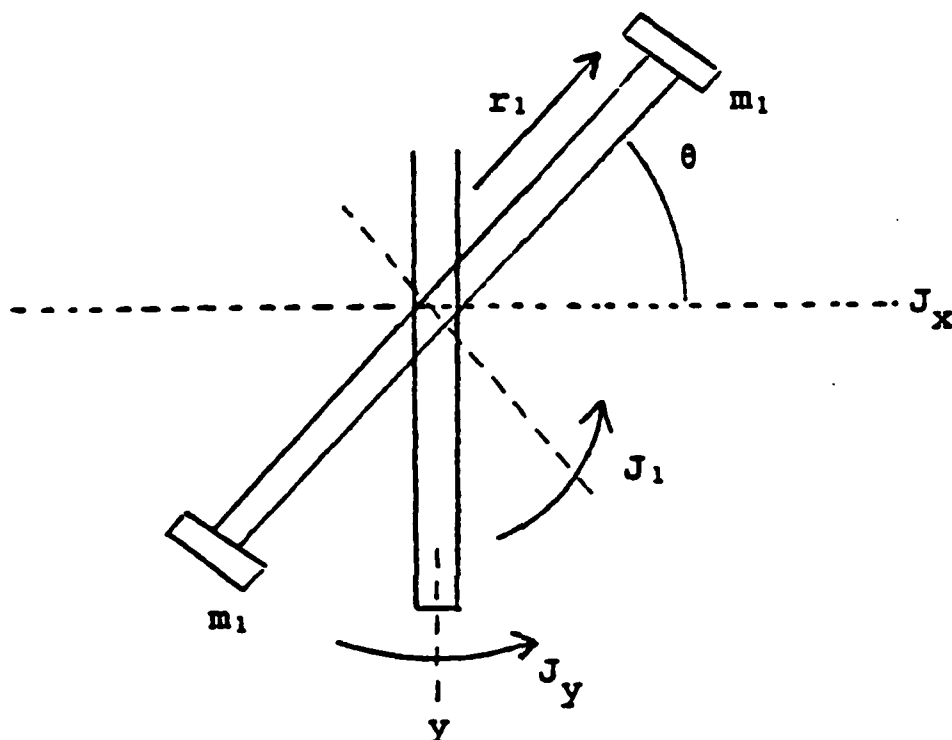
Also shown on the diagram is the RGyro. This is not a part of the plant. The RGyro defines an error associated with the roll axis. In earlier three gimbal gyros, the roll axis of the missile did not coincide with any of the gimbal axes. The four gimbal Mark 6 gyro aligns the roll axis with the outer gimbal axis, thus eliminating the need for the RGyro as an indication of gyro error. The output is still provided for ease in comparing current model errors with previous systems.

c. Gimbal Inertias

The gimbal inertias are represented in Figure 3.1 as J_S , J_I , J_M and J_O for the stable member and inner, middle and outer gimbals respectively. The outer and middle

Figure 3.1 Mark 6 Gyro Model (Inertial Mode).

gimbal inertias change with time as a function of the inner gimbal angle. Figure 3.2 shows how the inertias are resolved [Ref. 2: p. 6].



$$J_1 = r_1^2 m_1 \cos^2 \theta$$

resolving along the x and y axes:

$$J_x = I_{y^2} m_1 = r_1^2 m_1 \sin^2 \theta = J_o \sin^2 \theta$$

$$J_y = I_{x^2} m_1 = r_1^2 m_1 \cos^2 \theta = J_o \cos^2 \theta$$

for the four gimbal model:

$$J_M = J_M + J_I + J_S C_I^2$$

$$J_O = J_O + J_M + J_I C_M^2 + J_S C_M^2 S_I^2$$

Figure 3.2 Resolution of Outer and Middle Gimbal Inertias.

d. Stable Element

The stable member is represented by the upper flow path in Figure 3.1. There are no external inputs to the stable member, with only friction affecting the loop. The stable element is controlled by its own feedback loop and is not influenced by the other system signals. Signals from the stable loop do cross-couple to the other gimbals, however, with the torque command coupling to the middle and outer gimbals. The inertial rate S serves as an input to the stable member angle, shown at the bottom of the figure. This angle could also be shown connected to the stable element flow path, with an input from the outer gimbal inertial rate. Because the stable member is affected only by friction, it has not been included in the state-space model.

e. Sampling Rates

Two different sampling rates are used in the system. The U, V and W gyros are sampled at 300 Hz. The gimbal angles are sampled at 100 Hz.

f. Gimbal Lock Avoidance

The proximity of the system to gimbal lock can be measured by observing the sines of the inner and middle angles. The product $\text{SIN}(A_I) * \text{SIN}(A_M)$ gives an indication of how close the system is to gimbal lock, with gimbal lock occurring when the product equals one. The goal of gimbal lock avoidance is to drive the product of the sines to zero. This is accomplished by setting either the inner or middle angle to 0 or 180 degrees.

Only one angle need be controlled at a time. Figure 3.3 shows the regions where control would switch from one angle to another. This is based on the smallest of the absolute values of the sines.

The missile motion input to the U and V gyros has a gain factor of $\text{SIN}(A_M) * \text{SIN}(A_I)$, as seen in Figure 3.1. Thus, in addition to avoiding gimbal lock, nulling the

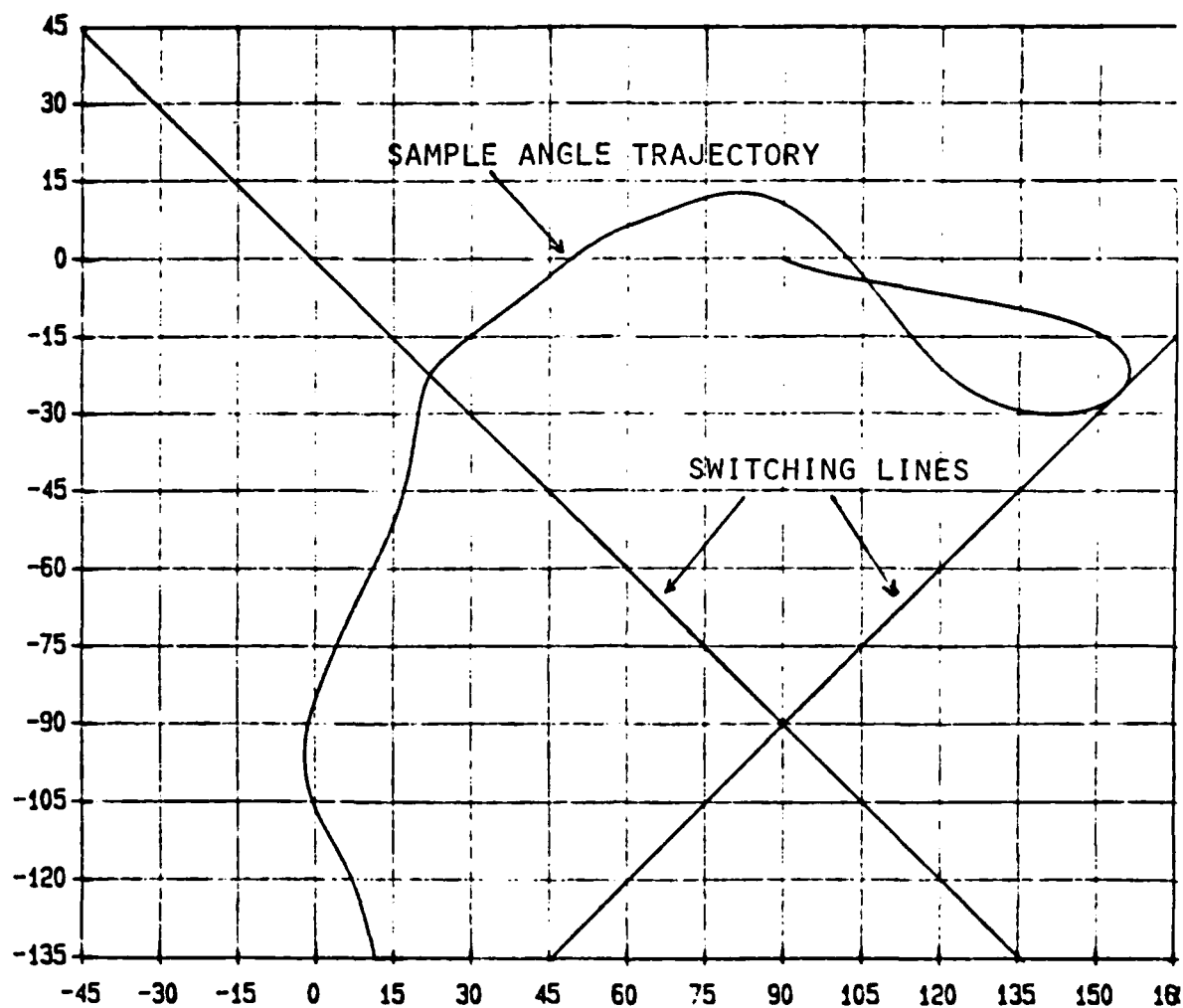


Figure 3.3 Gimbal Lock Avoidance Switching Line.

product of the sines of the inner and middle gimbal angles also minimizes the effect missile motion has on gyro error.

2. Gyro Controller

a. Control Laws

Figure 3.4 shows the controller for the Mark 6 gyro [Ref. 3: p. 115]. The six inputs to the controller are the three signals generated from the U,V and W gyros, the stable element gimbal angle and the sines of the inner and middle gimbal angles. The four outputs are the torque motor command signals.

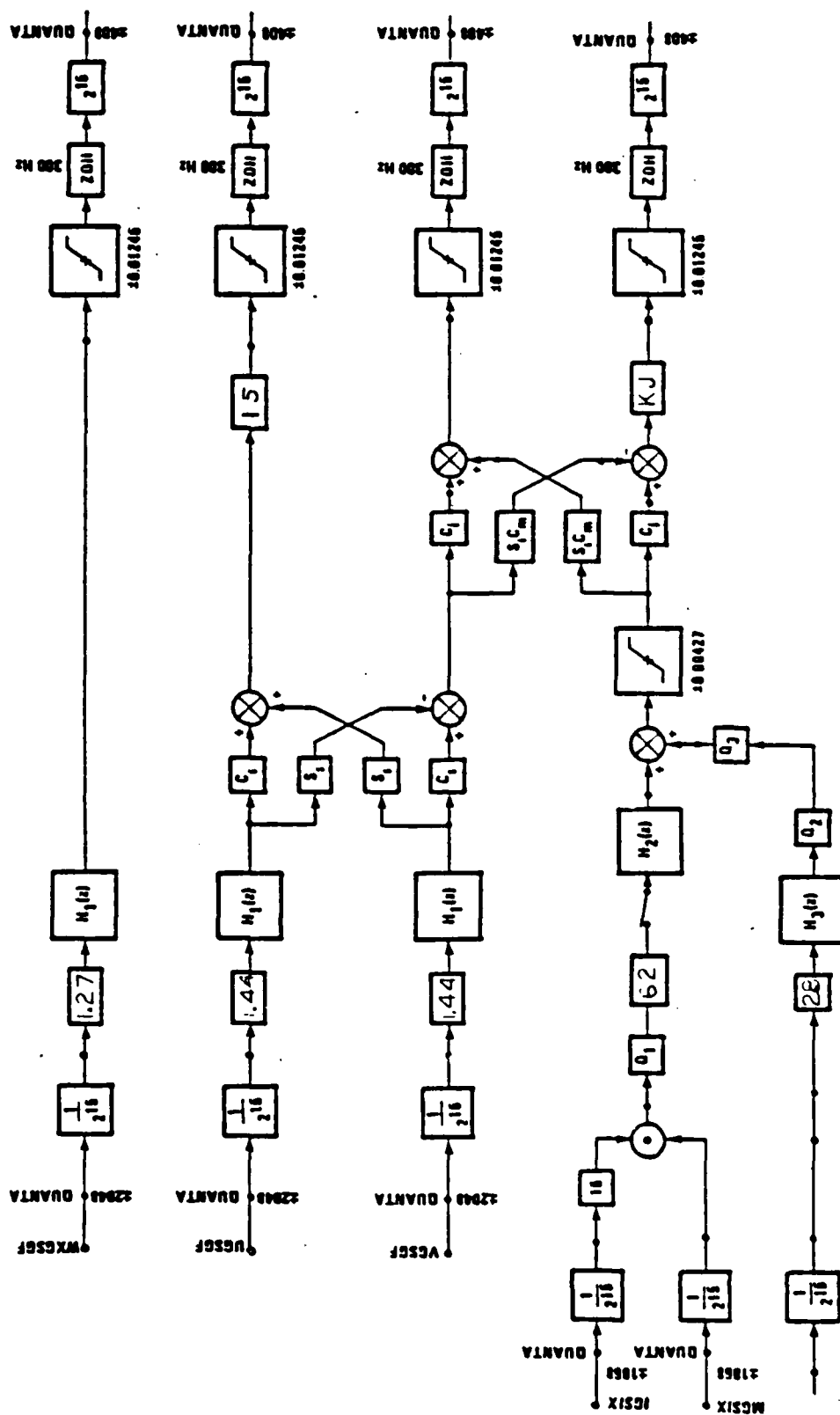


Figure 3.4 Mark 6 Gyro Control Law.

b. Transfer Functions

The transfer function $H_1(z)$ in the stable element, inner and middle gimbal feedback paths is defined as:

$$H_1(z) = (z-.932)^3(z-.80955)/(z-1)^2(z-.6186)(z-.17474)$$

The transfer functions $H_2(z)$ and $H_3(z)$ in the outer gimbal control loop are:

$$H_2(z) = (z-.9778)/(z+.3827)$$

$$H_3(z) = (z-1)/z$$

c. Redundant Torque

The outer gimbal control loop has three inputs controlled by switches Q_1, Q_2 and Q_3 . Two of the inputs are the $SIN(A_M)$ and $SIN(A_I)$ signals. The third input is the stable element angle. The two signals generated by this loop are necessary when the product $SIN(A_M)*SIN(A_I)$ becomes very small and does not produce a large enough error signal to drive the outer gimbal. Q_1 and Q_3 are switches with values of +1 and -1 depending on gimbal geometry. Switch Q_2 is closed for values of $SIN(A_M)*SIN(A_I)$ less than 1/8, and open for values greater than 1/8.

d. Scaling Factors

Gain blocks with 2^{15} and $1/2^{15}$ scaling factors are included in the control laws. These gain factors are applied in order to facilitate software processing of the feedback signals only.

IV. STATE-SPACE MODEL

A. BLOCK DIAGRAM

1. Plant Model

The state-space model of the Mark 6 Gyro is shown in Figure 4.1. Where appropriate, the gains from Figure 3.1 have been combined into a single block. Only the inner, middle and outer gimbals have been modeled. Eight states are identified on the figure.

2. Assumptions and Simplifications

A number of assumptions and simplifications have been made in order to develop the state-space model:

- (a) there is no friction (this eliminates the stable element loop)
- (b) all states are available for feedback
- (c) the inner and middle angles are fed back directly, not the sines of the angles
- (d) there are no limiters in the system
- (e) the entire system is sampled at 300 Hz

3. State-Space Equations

The state-space equations of the system are in the form:

$$\dot{x}(t) = A(t)x(t) + B(t)u(t)$$

The vectors $x(t)$ and $u(t)$ are described in Table I. $A(t)$ and $B(t)$ are the plant and control matrices, respectively. The matrices for this system are shown in Figure 4.2.

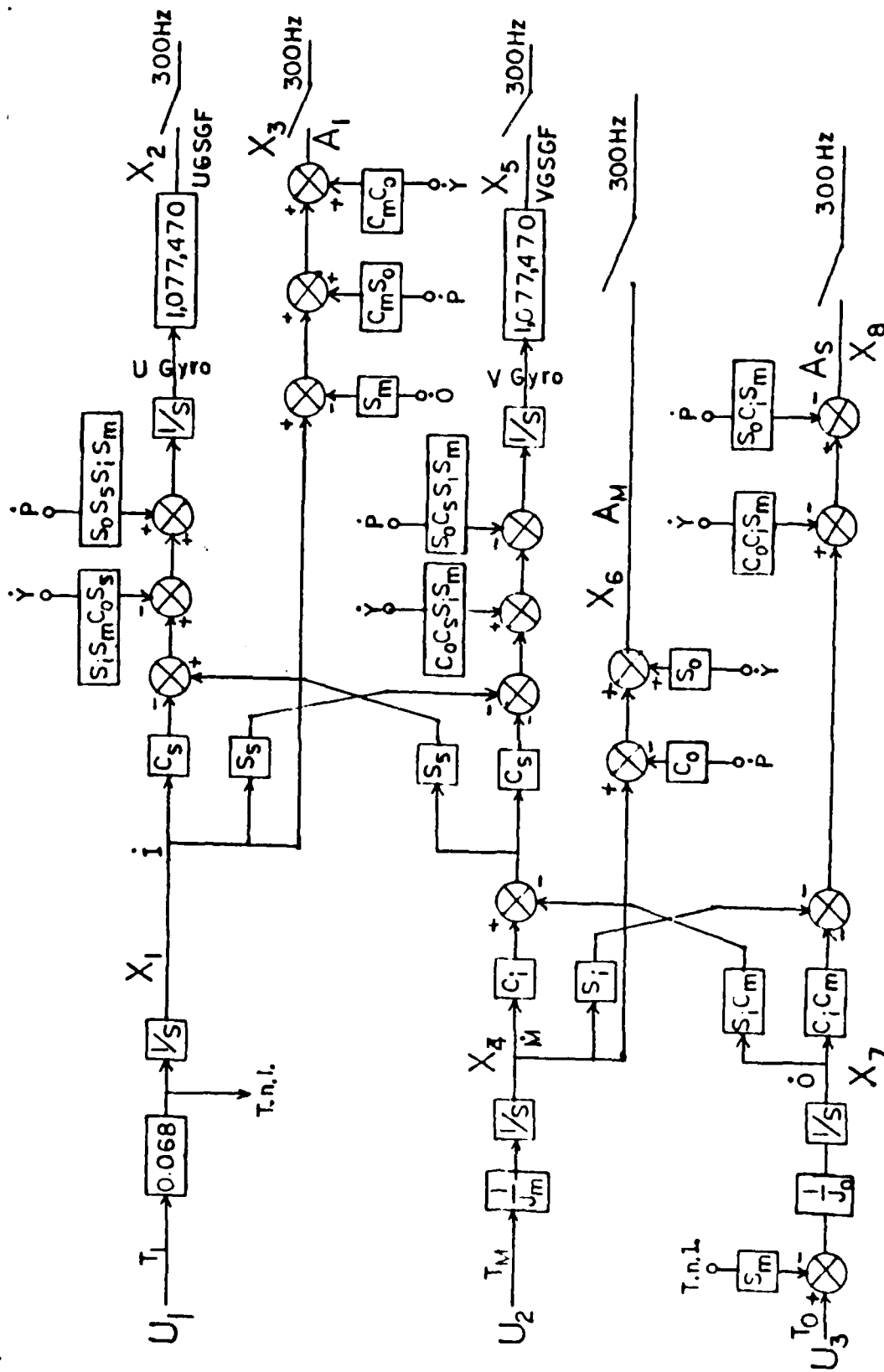


Figure 4.1 State-Space Model of the Mark 6 Gyro.

TABLE I
STATE AND CONTROL VECTORS

x_1	inner gimbal inertial rate I
x_2	U Gyro error
x_3	inner gimbal angle A_M
x_4	middle gimbal inertial rate M
x_5	V Gyro error
x_6	middle gimbal angle
x_7	outer gimbal inertial rate O
x_8	stable element gimbal angle
u_1	inner gimbal torque signal
u_2	middle gimbal torque signal
u_3	outer gimbal torque signal

Plant Matrix

$$\begin{bmatrix} 0 & 0 & 0 & 0 & 0 & 0 & 0 & 0 \\ -KC_S & 0 & 0 & KC_I S_S & 0 & 0 & -KS_I C_M S_S & 0 \\ 1 & 0 & 0 & 0 & 0 & 0 & 0 & -S_M \\ 0 & 0 & 0 & 0 & 0 & 0 & 0 & 0 \\ KS_S & 0 & 0 & -KC_I C_S & 0 & 0 & KC_S S_I C_M & 0 \\ 0 & 0 & 0 & 1 & 0 & 0 & 0 & 0 \\ 0 & 0 & 0 & 0 & 0 & 0 & 0 & 0 \\ 0 & 0 & 0 & -S_I & 0 & 0 & -C_I C_M & 0 \end{bmatrix}$$

where $K = 1,077,470$

Control Matrix

$$\begin{bmatrix} 0.068 & 0 & 0 \\ 0 & 0 & 0 \\ 0 & 0 & 0 \\ 0 & 1/J_M & 0 \\ 0 & 0 & 0 \\ 0 & 0 & 0 \\ -S_M/J_O & 0 & 1/J_O \\ 0 & 0 & 0 \end{bmatrix}$$

Figure 4.2 Plant and Control Matrices for State-Space Model.

V. OPTIMIZATION TECHNIQUE

A. OPTIMAL REGULATOR

1. Linear Quadratic Problem

The Mark 6 gyro model can be represented by the state differential equation

$$\dot{x}(t) = A(t)x(t) + B(t)u(t)$$

The goal of the optimization technique is to drive the system to the desired state as quickly as possible, while using only practical input amplitudes. The quadratic integral criterion can be used to express how rapid an initial state is driven to the final state [Ref. 4: p. 201]. This criterion can be expressed as:

$$J = \int x^T(t)R_3(t)x(t)dt$$

$R_3(t)$ is an appropriate weighting matrix chosen to minimize the output state vector. The criterion as represented above would require very large input amplitudes, usually unattainable in a practical system. Including the input in the quadratic integral yields

$$J = \int [x^T(t)R_3(t)x(t) + u^T(t)R_2(t)u(t)]dt$$

By proper selection of R_2 and R_3 , the output vector can be minimized using realizable input amplitudes.

Since only the controlled variables are of interest, the cost equation can be written in terms of the output vector $z(t)$, given as:

$$z(t) = D(t)x(t)$$

A weighting matrix R_1 can now be defined as:

$$R_1(t) = D^T(t)R_3(t)D(t)$$

$R_1(t)$ is a square, positive semi-definite symmetric matrix having the same order as the number of controlled variables of the system. The selection of the specific values for R_1 and R_2 are discussed in the next section.

The inputs for the Mark 6 gyro are the signals to the torque motors. These signals are generated solely as a function of gyro error and gimbal angular position. In the optimal regulator problem, the inputs can be expressed in terms of an optimal feedback gain matrix and the states.

$$u(t) = -Fx(t)$$

The state differential equation can then be written as:

$$\dot{x}(t) = A(t)x(t) + B(t)(-Fx(t)) + B(t)u_o(t)$$

When there are no external inputs, $u_o(t)=0$. Combining terms yields the following:

$$\dot{x}(t) = [A(t)-B(t)F(t)]x(t)$$

In the linear quadratic problem, the control law can be expressed as:

$$u(t) = -R_2^{-1}B^TPx(t)$$

The optimal feedback gain matrix now becomes:

$$F = R^{-1}B^TP$$

The matrix P is found by solving the Riccati equation:

$$PA + A^TP - PBR_2^{-1}B^TP + R_1 = 0$$

This is the solution for the steady-state optimal feedback gains, and is the method used to develop the feedback gain matrices used to control the Mark 6 gyro.

2. Choice of Weighting Matrices

The weighting matrices R_1 and R_2 were chosen based on the maximum values that the output vector and inputs could be expected to reach. When the weighting matrices have values only on the diagonal, the matrix product $x^T R x$ becomes x_i^2 / R_{ii} for each of the values of x . R_{ii} is then set equal to the inverse of the maximum expected value of x_i squared. This drives each of the terms in the cost equation to one when their value approaches the maximum allowed, and to zero when their value is small.

3. Non-zero Steady State Outputs

The solution to the linear quadratic optimal feedback gain problem has been outlined in the previous sections. This solution assumes, however, that the desired steady-state value of the controlled states is zero. Since the Mark 6 control law includes nulling the sine of the inner or middle angle, it is possible that the desired value of the inner or middle angle be 180 degrees, not 0. In this case, the optimal feedback gain control law becomes:

$$u(t) = -F[-R+x(t)]$$

The vector R here represents the reference signal in the system, as shown in Figure 5.1. When $R=0$, the optimal control solution reduces to that shown above.

In addition to an axis shift, driving the system to a non-zero set point can also be accomplished by adding a constant factor u_0 to the control input $u(t)$. The control input then becomes:

$$u(t) = -Fx(t) + u_0$$

A u_0 can be chosen such that when the system experiences a shift in the set point, as the gyro controller does when shifting from 0 to 180 degrees, an optimal response is obtained while remaining within allowable input amplitudes. [Ref. 4: pp.270-275].

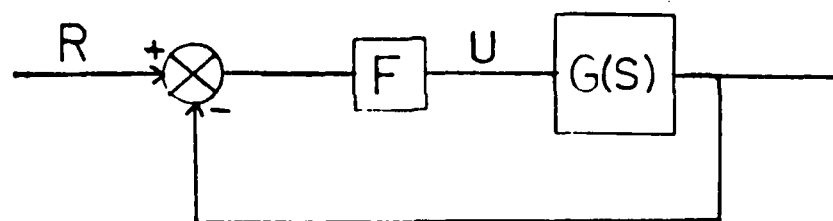


Figure 5.1 Optimal Gain Feedback Block Diagram.

This optimal constant input is defined as:

$$U_o = H_c^{-1}(0)z_o$$

In this equation, $H_c(s)$ is the closed loop transfer function from the inputs to the desired non-zero steady state output z_o . The use of this solution requires that the number of inputs is equal to the number of outputs, and that the inverse of transfer function $H_c(s)$ exists. If the transfer function has any zeros at the origin, the matrix $H_c(0)$ is singular and the inverse does not exist.

The optimal solution for the gyro controller generates one or more zeros at the origin depending on the particular gimbal angles. Thus, the optimal input u_o cannot be found and the axis shift technique must be used.

B. MARK 6 GYRO OPTIMAL CONTROLLER

1. Region Controller

With a sampling rate of 300 Hz, computing the optimal feedback gains every sampling interval would require an enormous amount of computations. Lauro has shown that a region controller will yield a nearly optimal response while greatly reducing the calculations involved [Ref. 1: p. 8].

The plant and control matrices of the Mark 6 gyro are a function of the gimbal angles, which in turn vary with time. The optimal regulator designed for the system divides the gimbal angle regions up into segments of 30 degrees or less. Optimal gains for the gimbal angles at the center of the region have been calculated. When the missile motion causes the gimbal angles to change from one region to another, the controller inserts the feedback gains calculated for that region. Figure 5.2 shows typical regional divisions for two angles. The regions are 10 degrees wide near zero, and 30 degrees wide further from the origin. The figure shows a two dimensional plot, although the actual gyro controller involves four angles in four dimensional space.

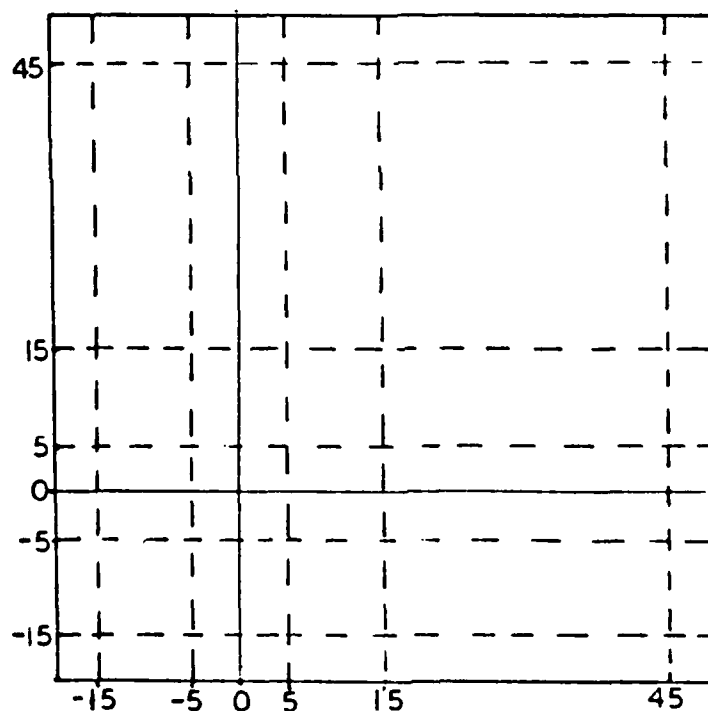


Figure 5.2 Region Controller Segments.

Figure 5.3 contains the algorithm of the computer program written to implement the optimal regulator. A copy of the program listing is included in Appendix C.

initialize missile motion and gyro rates to zero
assign initial gimbal angles
determine initial condition vector $x(0)$
 restrict all angles to ± 360 degrees
 determine optimal gain region based on gimbal angles
 assign appropriate optimal feedback gains
 calculate variable terms in plant and control matrices
 input missile motion
 calculate $x(k+1)$ values for each state

Figure 5.3 Algorithm for the Mark 6 Gyro Optimal Regulator.

VI. SYSTEM SIMULATION

A. SIMULATION MODEL

The model used for system simulation is a modified version of the state-space model shown in Figure 4.1. The U and V gyro errors are integrated, and the result nulled to minimize net gyro errors. The outer gimbal angle is calculated since it affects the plant and control matrices, but is not used for optimal feedback. The simulation model has eleven states, and is shown in Figure 6.1. The plant and control matrices for the simulation model are given in Figures 6.2 and 6.3.

B. WEIGHTING MATRICES

1. Torque Limits

Each axis of the gyro is driven by a torque motor. The amount of torque delivered by the motor is directly proportional to the feedback error signal. When the gyro errors are zero and the sine of the selected gimbal angle has been driven to null, no torque is generated.

The maximum torques which can be supplied to each axis are

- maximum inner axis torque $T_{I\max}$ 83 oz-in
- maximum middle axis torque $T_{M\max}$ 211 oz-in
- maximum outer axis torque $T_{O\max}$ 369 oz-in

Up to 14 percent more torque is available dependent upon the particular gimbal angles. This additional torque was not assumed to be available when designing the state-space system.

2. State Output Weighting Matrix R_1

The optimal control cost function is defined as

$$J = \int [z^T(t)R_1(t)z(t) + u^T(t)R_2(t)u(t)]dt$$

The output measurement vector $z(t)$ is

$$z(t) = [x_2(t) \ x_3(t) \ x_5(t) \ x_6(t) \ x_{10}(t) \ x_{11}(t)]^T$$

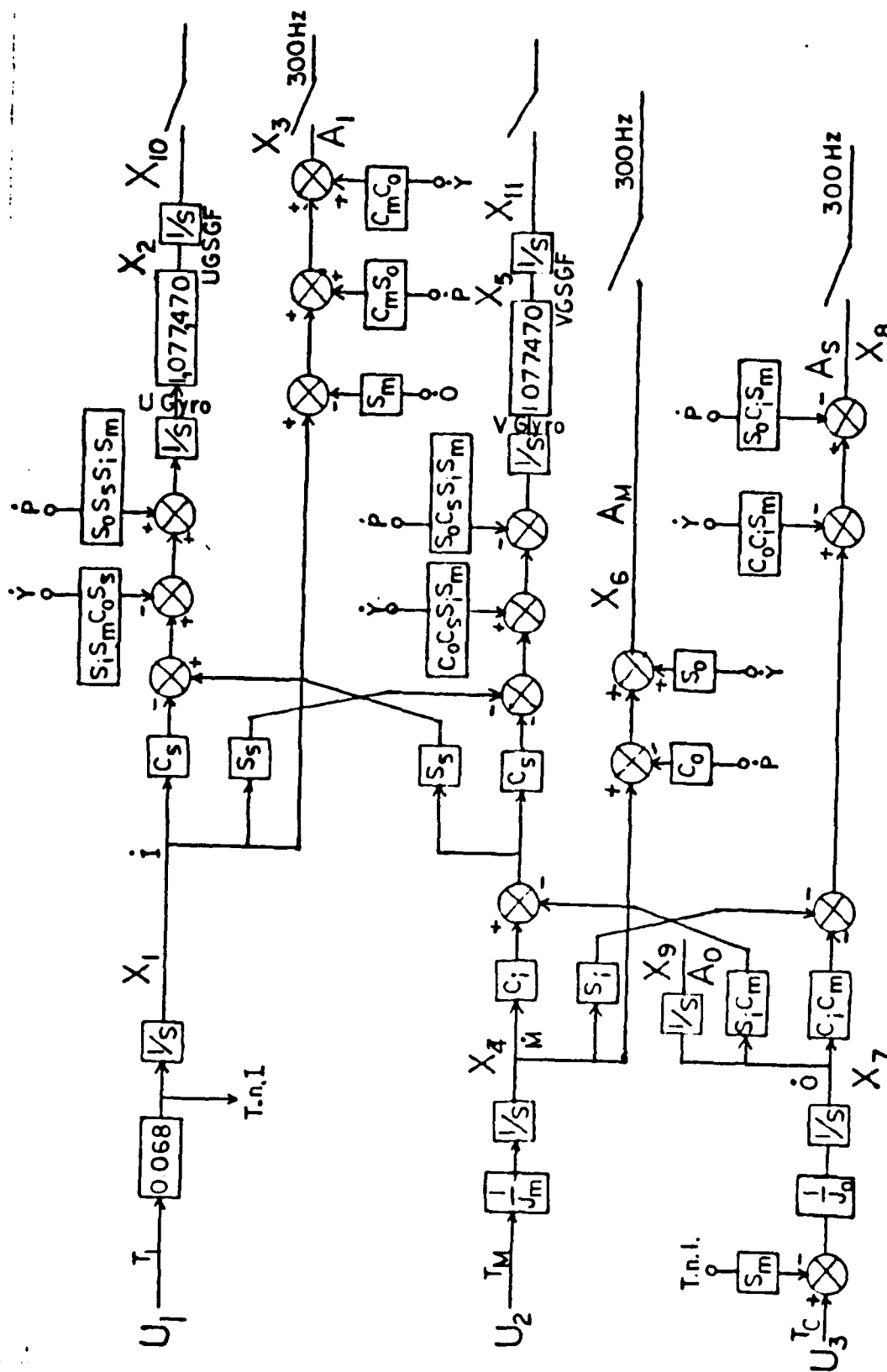


Figure 6.1 State-Space Simulation Model of the Mark 6 Gyro.

$$\begin{bmatrix} 0.068 & 0 & 0 \\ 0 & 0 & 0 \\ 0 & 0 & 0 \\ 0 & 1/J_M & 0 \\ 0 & 0 & 0 \\ 0 & 0 & 0 \\ -S_M/J_0 & 0 & 1/J_0 \\ 0 & 0 & 0 \\ 0 & 0 & 0 \\ 0 & 0 & 0 \\ 0 & 0 & 0 \end{bmatrix}$$

Figure 6.3 Control Matrix for the
State Space Simulation Model.

The output vector weighting matrix was chosen based on data provided by Draper Laboratory. The output vector varies with time depending on gimbal angles. The states which comprise the output vector and their maximum allowable values are shown in Table II.

TABLE II
OUTPUT STATE VECTOR MAXIMUM VALUES

x_2	U Gyro	300 quanta
x_3	inner gimbal angle	30 degrees
x_5	V Gyro	300 quanta
x_6	middle gimbal angle	30 degrees
x_{10}	V Gyro error integral	1
x_{11}	U Gyro error integral	1

The maximum value of 300 quanta listed for the gyro angles corresponds to an error of 0.278 milliradians. This

is the maximum error attained with the current Mark 6 gimbal model. It was desired to allow a smaller error in the state-space model. The gyro has a physical stop at 2048 quanta, or 1.9 milliradians. If the error reaches this value the system will fail.

The inner and middle gimbal angle maximum values were chosen as 30 degrees. This prevents the product $\text{SIN}(A_M)\text{SIN}(A_I)$ from exceeding 0.5.

The maximum value of the integrals of the U and V gyro errors was chosen arbitrarily as 1. This limit minimized gyro error without producing excessive input amplitudes.

The R_1 matrix in terms of the output variables is

$$R_1 = \begin{bmatrix} 1/(x_2)_o^2 & 0 & 0 & 0 & 0 & 0 \\ 0 & 1/(x_3)_o^2 & 0 & 0 & 0 & 0 \\ 0 & 0 & 1/(x_5)_o^2 & 0 & 0 & 0 \\ 0 & 0 & 0 & 1/(x_6)_o^2 & 0 & 0 \\ 0 & 0 & 0 & 0 & 1/(x_{10})_o^2 & 0 \\ 0 & 0 & 0 & 0 & 0 & 1/(x_{11})_o^2 \end{bmatrix}$$

Using the maximum values of the output states as given in Table II, The output cost matrix becomes

$$R_1 = \begin{bmatrix} 1.11 \times 10^{-5} & 0 & 0 & 0 & 0 & 0 \\ 0 & 3.65 & 0 & 0 & 0 & 0 \\ 0 & 0 & 1.11 \times 10^{-5} & 0 & 0 & 0 \\ 0 & 0 & 0 & 3.65 & 0 & 0 \\ 0 & 0 & 0 & 0 & 1 & 0 \\ 0 & 0 & 0 & 0 & 0 & 1 \end{bmatrix}$$

3. Control Input Weighting Matrix R_2

The control input weighting matrix is a third order symmetric matrix with the inverse of the square of the allowable torques, given previously, on the diagonal. The matrix is shown below. The inputs are related to the torques as follows:

- u_1 = inner axis torque T_I
- u_2 = middle axis torque T_M
- u_3 = outer axis torque T_O

$$R_2 = \begin{bmatrix} 1/(T_I)^2 & 0 & 0 \\ 0 & 1/(T_M)^2 & 0 \\ 0 & 0 & 1/(T_O)^2 \end{bmatrix}$$

Using the maximum torque values given previously, the R_2 matrix is:

$$R_2 = \begin{bmatrix} 1.45 \times 10^{-4} & 0 & 0 \\ 0 & 2.25 \times 10^{-5} & 0 \\ 0 & 0 & 7.34 \times 10^{-6} \end{bmatrix}$$

C. TEST PARAMETERS

1. Initial Conditions

The initial conditions used for the model simulation were provided by Draper Laboratory. This particular combination of initial conditions, along with the missile motion, has been determined to be the "worst case" situation for gyro control.

The gimbal angles have been initialized as follows:

- stable member gimbal angle - 0 degrees
- inner gimbal angle - 90 degrees
- middle gimbal angle - 0 degrees
- outer gimbal angle - 59.25 degrees

The system is started from rest, with all gimbal and angular rates zero. The initial condition vector $z(0)$ is:

$$\begin{aligned} x_1(0) &= 0 \\ x_2(0) &= 0 \\ x_3(0) &= 90 \text{ degrees} \\ x_4(0) &= 0 \\ x_5(0) &= 0 \\ x_6(0) &= 0 \\ x_7(0) &= 0 \end{aligned}$$

$$\begin{aligned}x_8(0) &= 0 \\x_9(0) &= 59.25 \text{ degrees} \\x_{10}(0) &= 0 \\x_{11}(0) &= 0\end{aligned}$$

2. Missile Motion

The missile motion used for the simulation is a pitch rate input. The input is applied at 8 rad/sec² to a steady-state value of 1.571 rad/sec, or 90 deg/sec. The input reaches steady-state after 0.19 seconds.

D. TEST RESULTS

The system was initialized using the values above, and the pitch input applied. The tabulated data for the simulation run is included in Appendix D.

Figure 6.4 shows a plot of U and V gyro error as a function of time. The switching points between optimal gain regions are shown on the figure. The error graphs show a transient error spike when the optimal gains are changed. The amplitude of this spike can be made arbitrarily small by reducing the size of the optimal control regions. If optimal gains were calculated and applied every sample interval, the curve would show no such fluctuations.

A comparison between the errors of the Draper lab Mark 6 model and the state-space model with optimal control region gains is shown in Figures 6.5 and 6.6. The UGSGF error signal, Figure 6.5, closely approximates the Draper model with the exception of the switching point transients. The error damps rapidly after the optimal gain change, maintaining a small steady state error. The pitch input to the U gyro has a gain including both the $\text{SIN}(A_M) * \text{SIN}(A_I)$ term and a $\text{SIN}(A_S)$ term, as seen in Figure 4.1. Since both the middle and stable gimbal angles are initially zero, the pitch rate does not affect the U gyro significantly at the start of the simulation run.

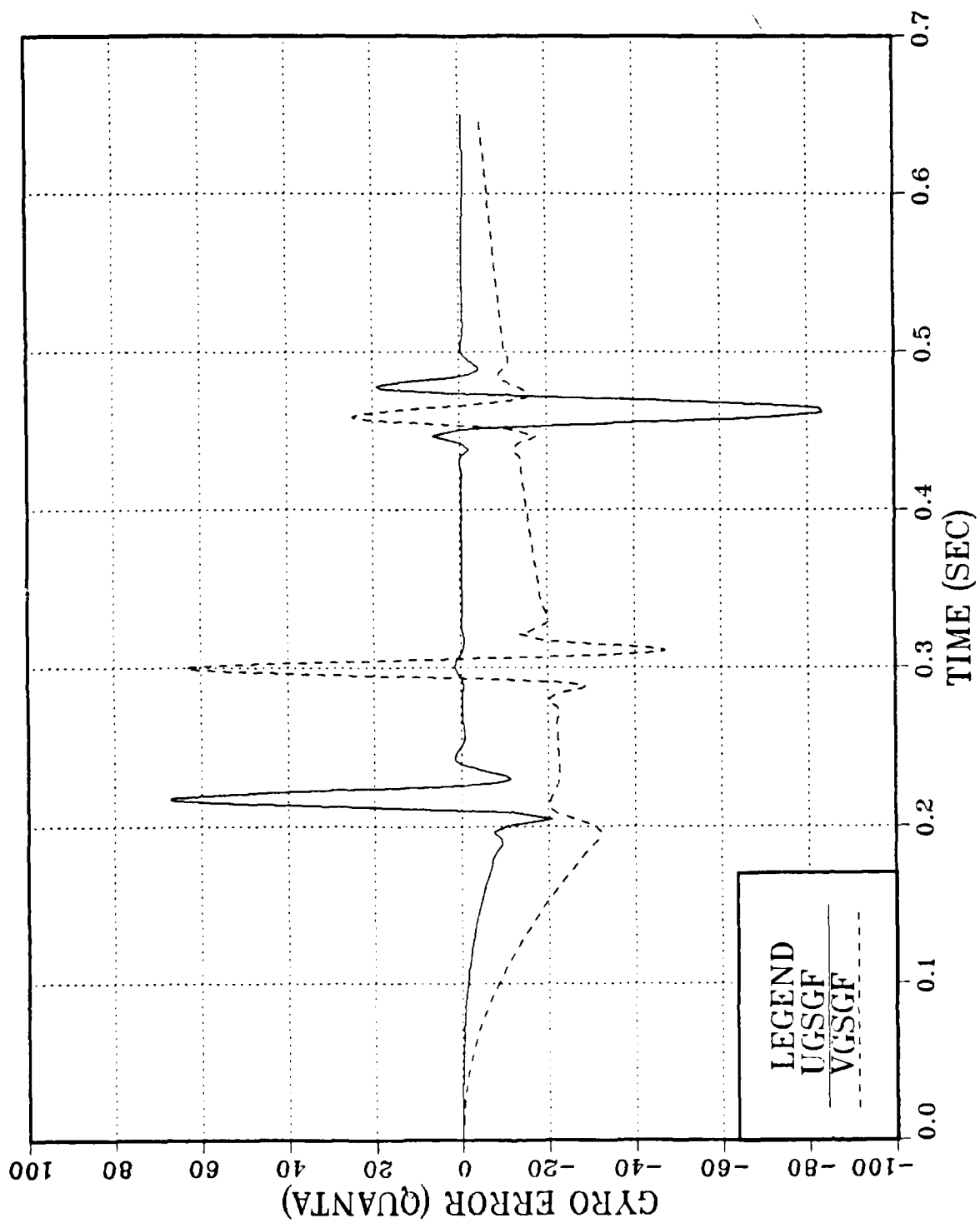


Figure 6.4 U and V gyro Errors for the State-Space Model.

The VGSGF error signal graph, Figure 6.6, shows a less pronounced response to missile motion than that experienced by the Draper model. The error transients again damp out quickly, with the system approaching but not attaining zero error at the end of the simulation run. The V gyro shows an immediate response to missile motion since the gain block contains a $\cos(A_S)$ term, allowing the pitch rate to affect the gyro error as soon as the middle gimbal angle moves away from zero.

The maximum gyro errors of the Draper lab model and the optimal model, neglecting the transient error spikes, are

- U gyro error Draper lab model 12 quanta
- U gyro error optimal model 10 quanta
- V gyro error Draper lab model 94 quanta
- V gyro error optimal model 31 quanta

The maximum transient errors of the optimal model are

- U gyro error 83 quanta
- V gyro error 63 quanta

Figure 6.7 compares the inner versus middle gimbal angle of the Draper model and the state-space model. The state-space model exhibits a more rapid middle gimbal angle change than the Draper model. The angular rate of the middle gimbal angle could be slowed down by varying the maximum allowed value of the angle in the R_2 weighting matrix. A slower angular rate would result in a smaller middle gimbal angle, and the $\sin(A_M)$ term in the gain path would reduce the effect the missile motion had on the U and V gyro errors. A trade-off between the two must be made, however, since the input signals required to hold the middle angle at a slower rate may adversely affect the gyro errors.

The inner gimbal angles of both systems translate at approximately the same rate. This can be expected since the sine of the middle angle, not the inner angle, is being nulled at the start of the simulation. The inner gimbal angle is not being controlled.

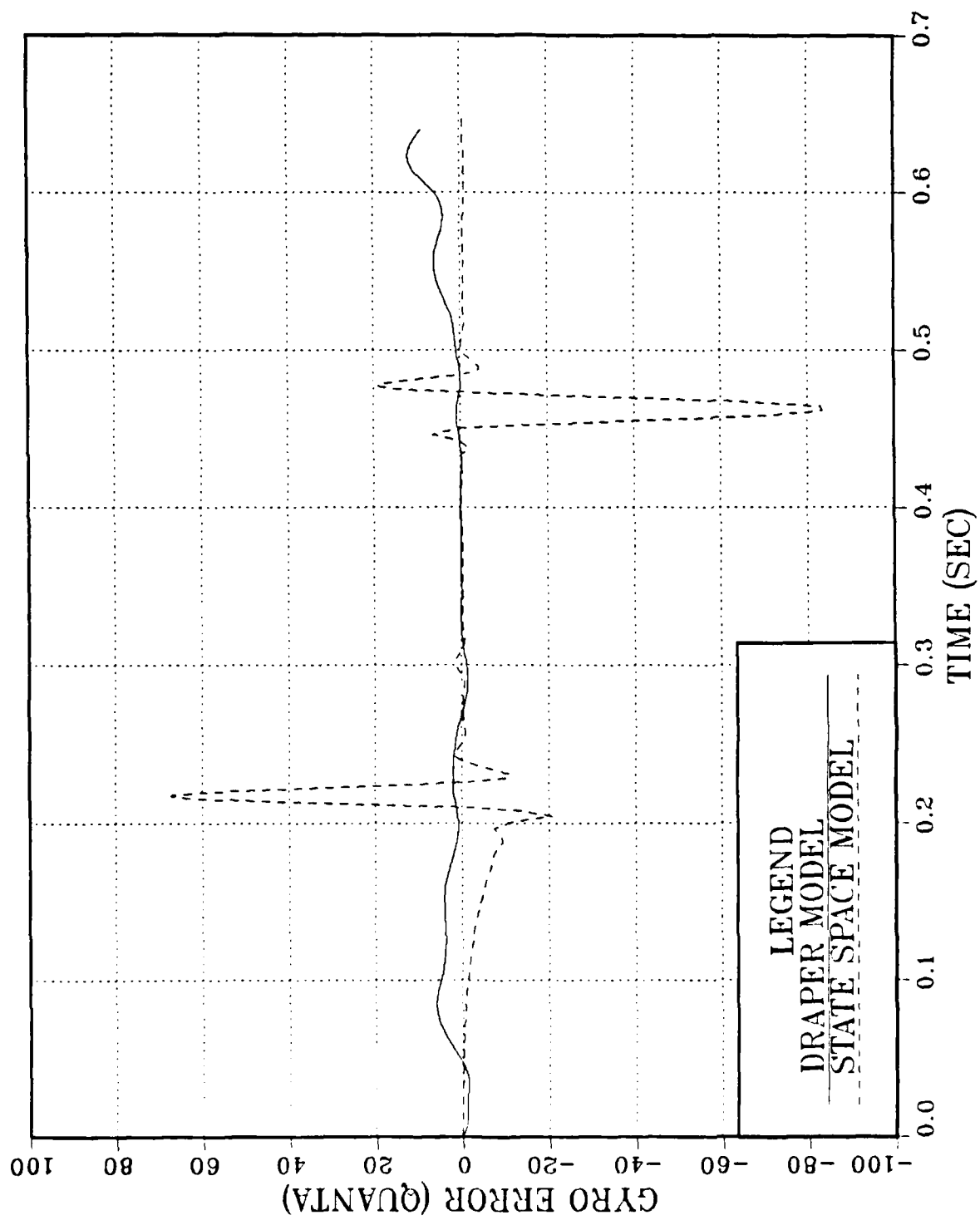


Figure 6.5 UGSGF Errors - Draper Lab and State-Space Models.

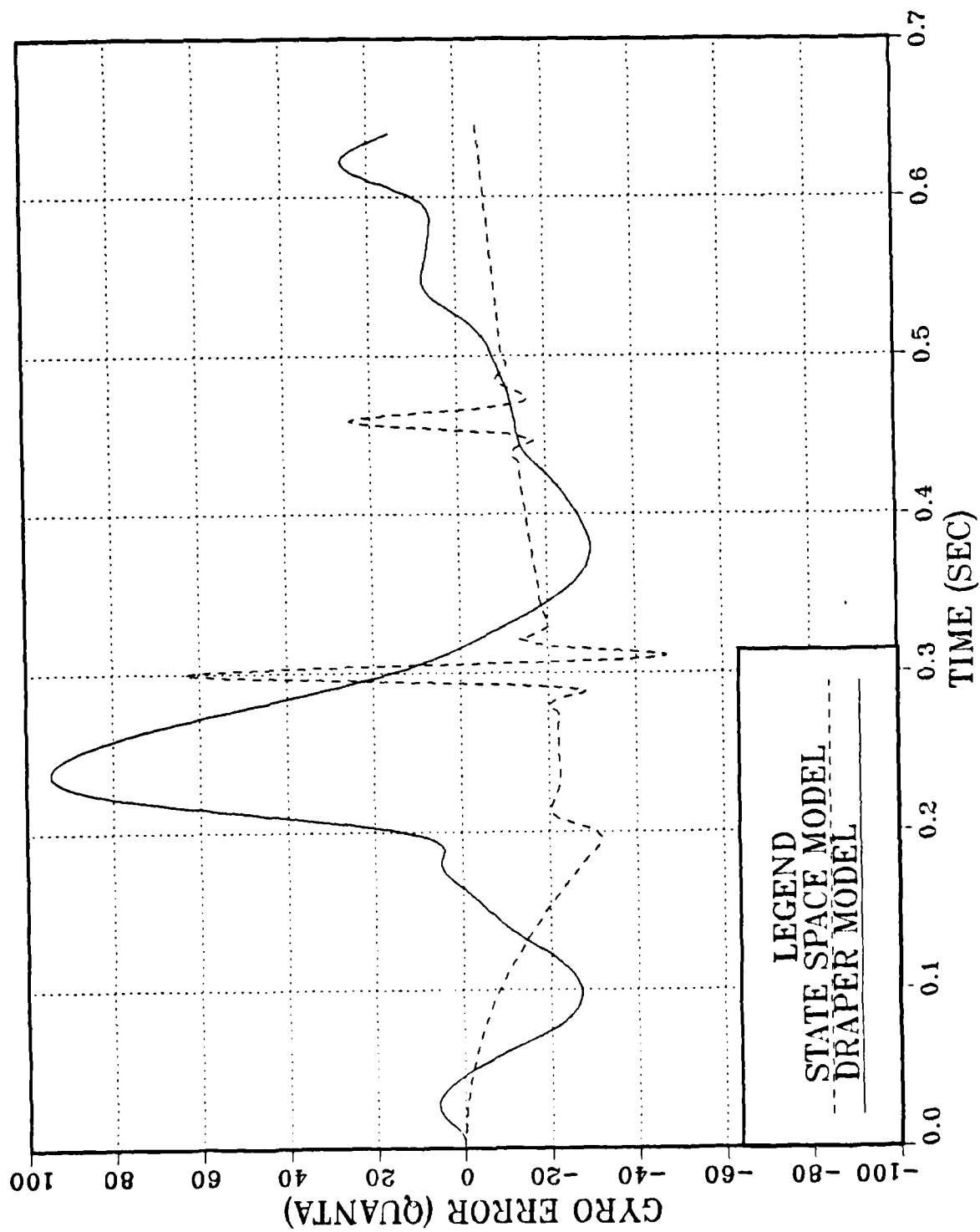


Figure 6.6 VGSGF Errors - Draper Lab and State-Space models.

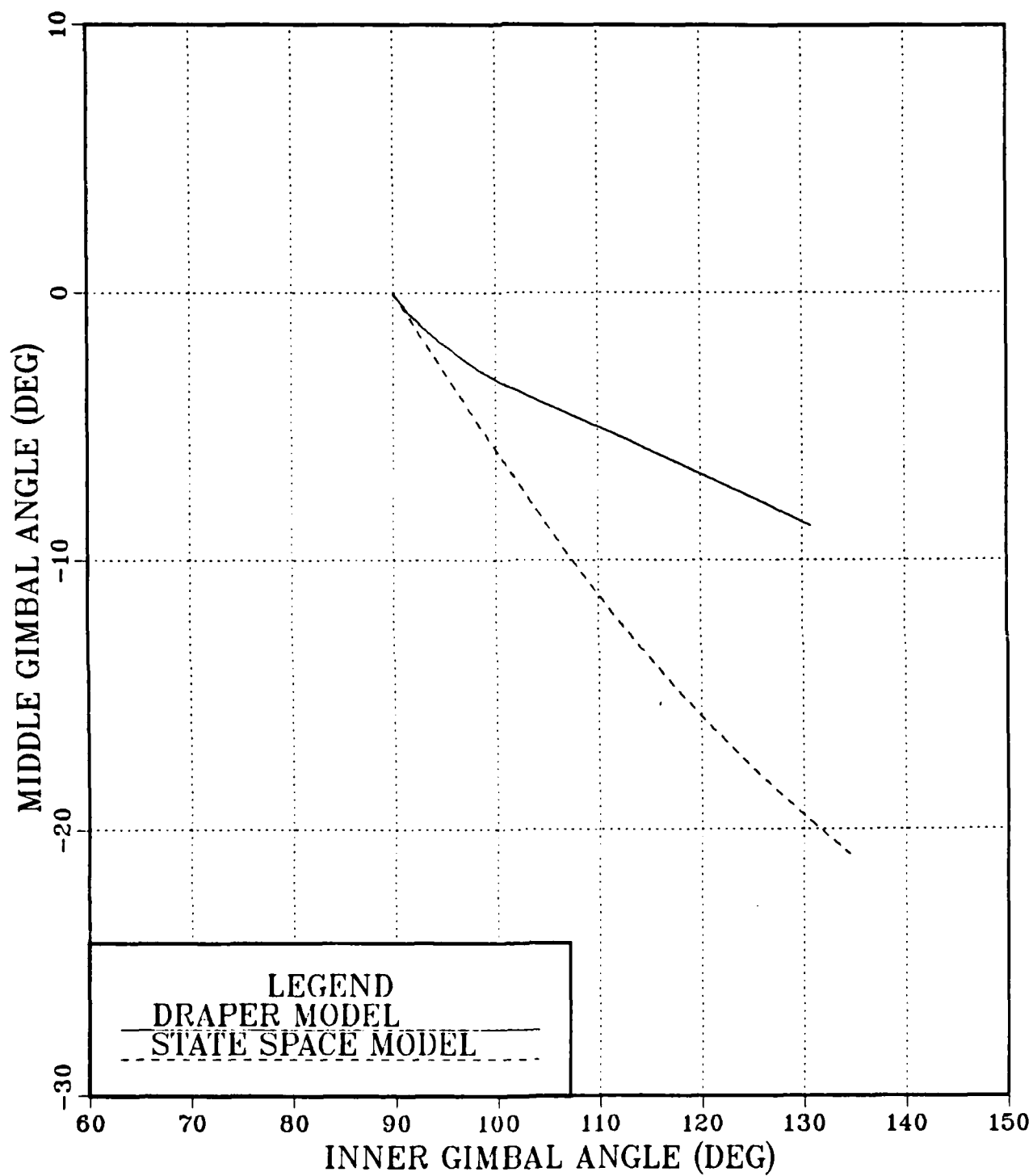


Figure 6.7 Inner and Middle Gimbal Angles.

VII. CONCLUSIONS AND RECOMMENDATIONS

A. CONCLUSIONS

1. Optimal Design Techniques

It has been shown that an optimal feedback gain controller can successfully control gyro errors and prevent gimbal lock. The unique, non-linear nature of the Mark 6 Gyro requires that several modifications be made to the linear quadratic problem solution.

As the gimbal angles vary, the internal plant gains vary. Depending on the gyro orientation, these gains can range from zero to one. Care must be taken in the regions surrounding zero gain, since the loop is effectively broken at this point. If the optimal control regions chosen are too large, the instantaneous switching of the gain from zero to a finite value may cause large transient errors from which the system is unable to recover. Narrowing the optimal control regions near the zero points will lessen the impact of the loop suddenly being closed. Increasing the number of control regions would also increase the memory size required to store the additional gain values. There exists a trade-off between system performance and the amount of control hardware required to implement the system.

The constantly changing gimbal angles also lead to numerous set point shifts. It was shown in chapter five that there exists an optimal control input which drives the state to the desired value without exceeding the input amplitude limitations. This solution requires that the inverse of the closed loop transfer function exists and that the number of controlled states is equal to the number of inputs. [Ref. 4: p. 279]. If either of these conditions is not met, a set point axis shift must be used, which may cause large transient errors. Narrowing the optimal control

regions in these areas may improve system performance. Again, additional memory space would be required.

B. RECOMMENDATIONS

1. Improving System Performance

The gyro controller used in the simulation was designed using the linear quadratic optimal feedback gain design technique. Since the technique provides optimal control only at the design point, a region controller will not provide optimal response to missile motion throughout the region. Changing the weighting matrices R_1 and R_2 for a particular region may provide improved system performance while still remaining within the allowable torque limits. Since the maximum allowable value for the controlled gimbal angle and gyro error integrals are essentially arbitrary, they can be varied and the resulting system performance analyzed to determine if the error in that region can be reduced.

The simulation model also neglected the effects of friction, which can reduce net torque to the axes by 3 to 4 oz-in. The friction effects, which are a function of gimbal angular rate, may produce a marked decrease in system performance in areas where the angles are changing rapidly.

Finally, the model assumed that all states were available for feedback and that there was no noise input. In practical applications, this assumption is invalid. A Kalman filter must be designed for the system to provide an estimate of the states which can not be measured, and to optimize system performance in the presence of both process and measurement noise. Harmonics from the gyros and the torque motors may have an effect on the system, along with structural noise generated during missile flight. The non-linearity and time varying nature of the system make the design of a filter particularly complex.

APPENDIX A
DEFINITIONS

TABLE III
VARIABLE DEFINITIONS

A_S	stable element gimbal angle
A_I	inner gimbal angle
A_M	middle gimbal angle
A_O	outer gimbal angle
\dot{S}	stable member inertial rate
\dot{I}	inner gimbal inertial rate
\dot{M}	middle gimbal inertial rate
\dot{O}	outer gimbal inertial rate
S_S	sine of stable element angle
C_S	cosine of stable element angle
S_I	sine of inner gimbal angle
C_I	cosine if inner gimbal angle
S_M	sine of middle gimbal angle
C_M	cosine of middle gimbal angle
S_O	sine of outer gimbal angle
C_O	cosine of outer gimbal angle
UGSGF	U gyro error signal expressed in quanta
VGSGF	V gyro error signal expressed in quanta
IMU	Inertial Measurement Unit the gyro and its controller

APPENDIX B

A

1. FOUR GIMBAL IMU MODEL

This appendix develops the equations which govern the gyro motion due to inputs from missile motion and torque motors. A block diagram of the plant is developed from the equations, which also leads to the state-space model [Ref. 2: pp. 2-7].

1. Assumptions and Approximations

This analysis includes the following assumptions and approximations:

- Spherical inertias
- Small torques due to gyroscopic effects

2. Definitions

Gimbal motion is positive in a clockwise direction. The transformation from an inner member to an outer member is then in the form:

$$\begin{array}{ccc} \text{inner member} & & \\ & C & = \\ \text{outer member} & & \end{array} \begin{bmatrix} \cos & -\sin & 0 \\ \sin & \cos & 0 \\ \cos & 0 & 1 \end{bmatrix}$$

- Standard i, j, k axes will be used.
- x, y and z are rate components on the i, j and k axes.
- p, q and r are body, or missile, motion rates on the i, j and k axes representing pitch, roll and yaw respectively.
- A positive torque T applied to a gimbal causes a positive, clockwise rotation.
- Ex, Ey and Ez are the gyro errors sensed on the stable, or inertial, member.

3. Symbols

- \dot{S} - Stable member gimbal rate resulting from applied torque
- \dot{I} - Inner member gimbal rate resulting from applied torque
- \dot{M} - Middle member gimbal rate resulting from applied torque
- \dot{O} - Outer member gimbal rate resulting from applied torque
- \dot{A}_s - Stable member gimbal rate resulting from relative motion between gimbals
- \dot{A}_i - Inner member gimbal rate resulting from relative motion between gimbals
- \dot{A}_m - Middle member gimbal rate resulting from relative motion between gimbals
- \dot{A}_o - Outer member gimbal rate resulting from relative motion between gimbals

4. Transformation of missile motion to inertial member

a. Base motion

$$\text{Base motion } W_b(5) = p_{i5} + q_{j5} + r_{k5}$$

referred to outer gimbal: (degree of freedom along j_4 and j_5)

$$\left. \begin{matrix} W_b \\ 0 \end{matrix} \right| = \begin{bmatrix} C_o & 0 & -S_o \\ 0 & 1 & 0 \\ S_o & 0 & C_o \end{bmatrix} \begin{matrix} p \\ q \\ r \end{matrix}$$

$$\left. \begin{matrix} W_{bx} \\ W_{by} \\ W_{bz} \end{matrix} \right|_{O(4)} = \begin{bmatrix} C_o * p - S_o * r \\ q \\ S_o * p + C_o * r \end{bmatrix}$$

Rates along W_{by} do not couple to outer gimbal. O is a rate applied to the outer gimbal from its torque motor.

$$\begin{matrix} W_{ox} \\ W_{oy} \\ W_{oz} \end{matrix} \bigg|_{0(4)} = \begin{bmatrix} Co*p - So*r \\ 0 \\ So*p + Co*r \end{bmatrix}$$

b. Outer gimbal to middle gimbal transformation

Referred to middle gimbal: (degree of freedom along the i3 and i4 axes)

$$\begin{matrix} W_{ox} \\ W_{oy} \\ W_{oz} \end{matrix} \bigg|_{M(3)} = \begin{bmatrix} 1 & 0 & 0 \\ 0 & Cm & -Sm \\ 0 & Sm & Cm \end{bmatrix} \begin{bmatrix} Co*p - So*r \\ 0 \\ So*p + Co*r \end{bmatrix}$$

$$= \begin{bmatrix} Co*p - So*r \\ Cm*0 - Sm(So*p + Co*r) \\ Sm*0 + Cm(So*p + Co*r) \end{bmatrix}$$

Rates along $W_{ox|m}$ do not couple to middle gimbal. M is the rate of middle gimbal applied by its torque motor.

$$\begin{matrix} W_{mk} \\ W_{my} \\ W_{mz} \end{matrix} \bigg|_{M(3)} = \begin{bmatrix} M \\ Cm*0 - Sm*(So*p + Co*p) \\ Sm*0 + Cm*(So*p + Co*r) \end{bmatrix}$$

c. Middle gimbal to inner gimbal transformation.

Referred to inner gimbal (degree of freedom along k2 and k3 axes):

$$\begin{matrix} W_{mx} \\ W_{my} \\ W_{mz} \end{matrix} \bigg|_{I(2)} = \begin{bmatrix} C_i & -S_i & 0 \\ S_i & C_i & 0 \\ 0 & 0 & 1 \end{bmatrix} \begin{bmatrix} M \\ C_m*O - S_m*(S_o*p + C_o*r) \\ S_m*O + C_m*(S_o*p + C_o*r) \end{bmatrix}$$

$$= \begin{bmatrix} C_i*m - S_i*''C_m*O - S_m*(S_o*p + C_o*r)' \\ S_i*m + C_i*EC_m*O - S_m*(S_o*p + C_o*r)T \\ S_m*O + C_m*(S_o*p + C_o*r) \end{bmatrix}$$

Rates along $W_{mz}|I$ do not couple into inner gimbal. I is rate on inner gimbal applied by torque motor, therefore:

$$\begin{matrix} W_{ix} \\ W_{iy} \\ W_{iz} \end{matrix} \bigg|_{I(2)} = \begin{bmatrix} C_i*M - S_i*EC_m*O - S_m*(S_o*p + C_o*r)T \\ S_i*M + C_i*EC_m*O - S_m*(S_o*p + C_o*r)T \\ I \end{bmatrix}$$

d. Inner gimbal to stable member transformation.

Referred to stable member (degree of freedom along j_1 and j_2 axes):

$$\begin{matrix} W_{ix} \\ W_{iy} \\ W_{iz} \end{matrix} \bigg|_{S(1)} = \begin{bmatrix} C_s & 0 & -S_s \\ 0 & 1 & 0 \\ S_s & 0 & C_s \end{bmatrix} \begin{bmatrix} W_{ix} \\ W_{iy} \\ W_{iz} \end{bmatrix}$$

$$= \begin{bmatrix} C_s*W_{ix} - S_s*W_{iz} \\ W_{iy} \\ S_s*W_{ix} + C_s*W_{iz} \end{bmatrix}$$

Rates along $W_{iy}|s$ do not couple across. E is rate on stable member applied by motor, therefore:

$$\begin{array}{c} W_{ex} \\ W_{ey} \\ W_{ez} \end{array} \left| \begin{array}{c} \\ \\ S \end{array} \right. = \begin{bmatrix} Cs*[Ci*M - Si*[Cm*O - Sm*(So*p + Co*r)]] - Ss*I \\ E \\ Ss*[Ci*M - Si*[Cm*O - Sm*(So*p + Co*r)]] + Cs*I \end{bmatrix}$$

e. Four Gimbal Block Diagram.

The following expressions are used to develop the four gimbal IMU block diagram shown in Figure B.1:

$$\dot{A}_E = W_{EYj1} - W_{IYj2}$$

$$\dot{A}_I = W_{IZk2} - W_{MZk3}$$

$$\dot{A}_M = W_{MXi3} - W_{OXi4}$$

$$\dot{A}_O = W_{OYj4} - W_{BYj5}$$

$$E_Y = E_{j1}$$

$$E_X = W_{EXi1}$$

$$E_Z = W_{EZk1}$$

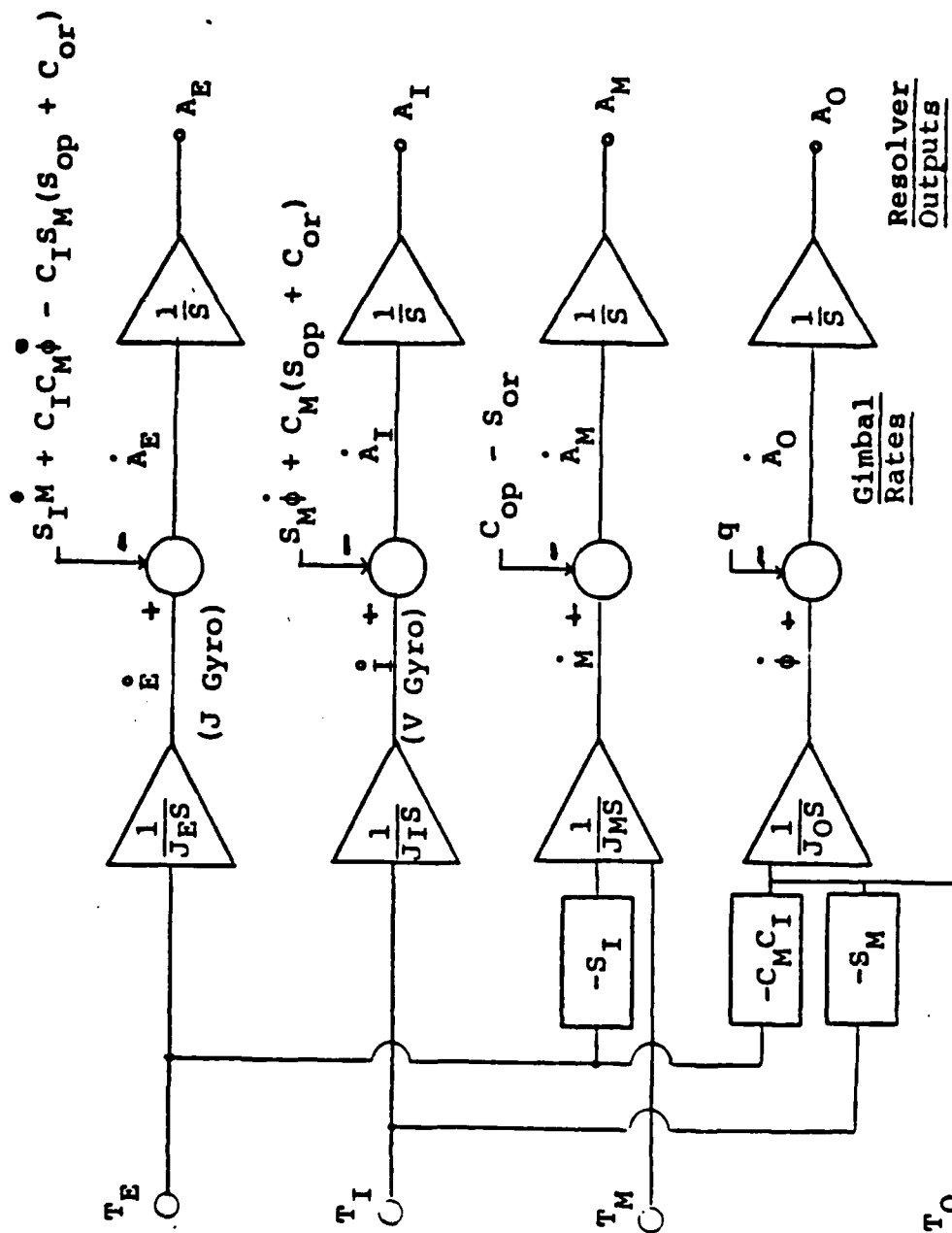


Figure B.1 Four Gimbal Gyro Block Diagram.

[illegible]

```

C      ASSIGN INITIAL CONDITION VECTOR
X1(1)=0
X2(1)=0
X3(1)=ANGI
X4(1)=0
X5(1)=0
X6(1)=ANGM
X7(1)=0
X8(1)=ANGS
X9(1)=ANGO
X10(1)=0
X11(1)=0

CCC
P=0
T=0.00033333
TWOPI=6.283185308
PI=3.14159

CCCC STEP THROUGH ROUTINE 2800 TIMES

CCCC DO 10 K=1,2800

CCCC RESTRICT GIMBAL ANGLES TO BETWEEN -360 AND +360

1      IF (X3(K).GE.TWOPI) THEN
        X3(K)=X3(K)-TWOPI
        IF (X3(K).GE.TWOPI) GO TO 1
        ELSE IF (X3(K).LE.-TWOPI) THEN
        X3(K)=X3(K)+TWOPI
        IF (X3(K).LE.-TWOPI) GO TO 1
        END IF
        IF (X6(K).GE.TWOPI) THEN
        X6(K)=X6(K)-TWOPI
        IF (X6(K).GE.TWOPI) GO TO 2
        ELSE IF (X6(K).LE.-TWOPI) THEN
        X6(K)=X6(K)+TWOPI
        IF (X6(K).LE.-TWOPI) GO TO 2
        END IF
        IF (X8(K).GE.TWOPI) THEN
        X8(K)=X8(K)-TWOPI
        IF (X8(K).GE.TWOPI) GO TO 3
        ELSE IF (X8(K).LE.-TWOPI) THEN
        X8(K)=X8(K)+TWOPI
OPT00490
OPT00500
OPT00510
OPT00520
OPT00530
OPT00540
OPT00550
OPT00560
OPT00570
OPT00580
OPT00590
OPT00600
OPT00610
OPT00620
OPT00630
OPT00640
OPT00650
OPT00660
OPT00670
OPT00680
OPT00690
OPT00700
OPT00710
OPT00720
OPT00730
OPT00740
OPT00750
OPT00760
OPT00770
OPT00780
OPT00790
OPT00800
OPT00810
OPT00820
OPT00830
OPT00840
OPT00850
OPT00860
OPT00870
OPT00880
OPT00890
OPT00900
OPT00910
OPT00920
OPT00930
OPT00940
OPT00950
OPT00960

```

```

OPT00970
OPT00980
OPT00990
OPT01000
OPT01010
OPT01020
OPT01030
OPT01040
OPT01050
OPT01060
OPT01070
OPT01080
OPT01090
OPT01100
OPT01110
OPT01120
OPT01130
OPT01140
OPT01150
OPT01160
OPT01170
OPT01180
OPT01190
OPT01200
OPT01210
OPT01220
OPT01230
OPT01240
OPT01250
OPT01260
OPT01270
OPT01280
OPT01290
OPT01300
OPT01310
OPT01320
OPT01330
OPT01340
OPT01350
OPT01360
OPT01370
OPT01380
OPT01390
OPT01400
OPT01410
OPT01420
OPT01430
OPT01440

IF (X8(K).LE.-TWOPI) GO TO 3
END IF
IF (X9(K).GE.TWOPI) THEN
  X9(K)=X9(K)-TWOPI
  IF (X9(K).GE.TWOPI) GO TO 4
ELSE IF (X9(K).LE.-TWOPI) THEN
  X9(K)=X9(K)+TWOPI
  IF (X9(K).LE.-TWOPI) GO TO 4
END IF
PUT ANGLES IN DEGREES FOR OPTIMAL GAIN SELECTION

ANGS=X8(K)*180/PI
ANGI=X3(K)*180/PI
ANGW=X6(K)*180/PI
ANGO=X9(K)*180/PI

ASSIGN OPTIMAL GAINS BASED ON GIMBAL ANGLES
*****
ROUTINE TO DETERMINE IF SIN AI OR SIN AM SHOULD BE NULLED
R=0
TEST=0
TEMP1=ABS(SM)
TEMP2=ABS(SI)
IF (TEMP2.LT.TEMP1) THEN
  TEST=1
  GO TO 444
ENDIF
*****
C*****
F110=0
F210=0
F310=0
C
IF (ANGO.LT.45) GO TO 999
IF { ANGO.GE.45 .AND. ANGO.LE.75 } GO TO 1000
IF { ANGO.GT.75 } GO TO 999
C*****
C*****
1000 IF { ANGS.LT.-45 } GO TO 999
IF { ANGS.GE.-45 .AND. ANGS.LT.-15 } GO TO 1200
IF { ANGS.GE.-15 .AND. ANGS.LE.15 } GO TO 1100
IF { ANGS.GT.15 } GO TO 999
C*****
C*****
OPT01430
OPT01440
```



```

C 1100 IF { ANGM. LT. -45) GO TO 999
      IF { ANGM. GE. -45 .AND. ANGM. LT. -22.5) GO TO 1140
      IF { ANGM. GE. -22.5 .AND. ANGM. LT. -15) GO TO 1130
      IF { ANGM. GE. -15 .AND. ANGM. LT. -5) GO TO 1120
      IF { ANGM. GE. -5 .AND. ANGM. LE. 5) GO TO 1110
      IF { ANGM. GT. 5) GO TO 999
C *****
C 1110 IF { ANGI. LT. 75) GO TO 999
      IF { ANGI. GE. 75 .AND. ANGI. LE. 105) GO TO 1111
      IF { ANGI. GE. 105 .AND. ANGI. LT. 135) GO TO 1112
      IF { ANGI. GT. 135) GO TO 999
C *****
C 1120 IF { ANGI. LT. 75) GO TO 999
      IF { ANGI. GE. 75 .AND. ANGI. LT. 105) GO TO 1122
      IF { ANGI. GE. 105 .AND. ANGI. LT. 135) GO TO 1121
      IF { ANGI. GE. 135) GO TO 999
C *****
C 1130 IF { ANGI. LT. 105) GO TO 999
      IF { ANGI. GE. 105 .AND. ANGI. LT. 135) GO TO 1131
      IF { ANGI. GE. 135 .AND. ANGI. LT. 165) GO TO 1132
      IF { ANGI. GE. 165) GO TO 999
C *****
C 1140 IF { ANGI. LT. 135) GO TO 999
      IF { ANGI. GE. 135 .AND. ANGI. LT. 165) GO TO 1141
      IF { ANGI. GE. 165) GO TO 999
C *****
C 1200 IF { ANGM. LT. -45) GO TO 999
      IF { ANGM. GE. -45 .AND. ANGM. LT. -15) GO TO 1210
      IF { ANGM. GE. -15 .AND. ANGM. LT. -5) GO TO 1220
      IF { ANGM. GT. -5) GO TO 999
C *****
C 1210 IF { ANGI. LT. 135) GO TO 999
      IF { ANGI. GE. 135 .AND. ANGI. LT. 165) GO TO 1211
      IF { ANGI. GT. 165) GO TO 999
C *****

```

OPT01450
OPT01460
OPT01470
OPT01480
OPT01490
OPT01500
OPT01510
OPT01520
OPT01530
OPT01540
OPT01550
OPT01560
OPT01570
OPT01580
OPT01590
OPT01600
OPT01610
OPT01620
OPT01630
OPT01640
OPT01650
OPT01660
OPT01670
OPT01680
OPT01690
OPT01700
OPT01710
OPT01720
OPT01730
OPT01740
OPT01750
OPT01760
OPT01770
OPT01780
OPT01790
OPT01800
OPT01810
OPT01820
OPT01830
OPT01840
OPT01850
OPT01860
OPT01870
OPT01880
OPT01890
OPT01900
OPT01910
OPT01920

OPT02410
 OPT02420
 OPT02430
 OPT02440
 OPT02450
 OPT02460
 OPT02470
 OPT02480
 OPT02490
 OPT02500
 OPT02510
 OPT02520
 OPT02530
 OPT02540
 OPT02550
 OPT02560
 OPT02570
 OPT02580
 OPT02590
 OPT02600
 OPT02610
 OPT02620
 OPT02630
 OPT02640
 OPT02650
 OPT02660
 OPT02670
 OPT02680
 OPT02690
 OPT02700
 OPT02710
 OPT02720
 OPT02730
 OPT02740
 OPT02750
 OPT02760
 OPT02770
 OPT02780
 OPT02790
 OPT02800
 OPT02810
 OPT02820
 OPT02830
 OPT02840
 OPT02850
 OPT02860
 OPT02870
 OPT02880

F19=0. 134149E+02
 F21=-. 1533123E+02
 F22=0. 303621E-07
 F23=0. 134458E-04
 F24=0. 517502E+01
 F25=0. 487442E+01
 F26=0. 00000E+00
 F27=0. 943919E+04
 F28=0. 178897E-23
 F29=0. 118859E+04
 F31=-. 127164E+03
 F32=0. 778576E-02
 F33=0. 124747E-07
 F34=0. 136002E+05
 F35=0. 124995E+02
 F36=0. 00000E+00
 F37=0. 239397E+05
 F38=0. 536589E-23
 F39=0. 304791E+04
 CO TO 50
 ANGS=0 ANCI=120 ANCM=-10 ANCO=60
 F11=0. 790490E+04
 F12=-. 196716E+01
 F13=-. 714125E-21
 F14=0. 222004E+02
 F15=0. 247746E-01
 F16=0. 00000E+00
 F17=0. 378681E+02
 F18=-. 748735E-38
 F19=0. 555408E+01
 F110=-. 262554E+03
 F21=-. 332298E+03
 F22=0. 723837E-01
 F23=-. 445311E-15
 F24=0. 368703E+04
 F25=0. 227908E+01
 F26=0. 00000E+00
 F27=0. 628910E+04
 F28=-. 751346E-32
 F29=0. 376893E+03
 F210=0. 797282E+01
 F31=-. 848588E+03
 F32=0. 184846E+00
 F33=0. 534540E-15
 F34=0. 941557E+04
 F35=0. 582010E+01
 F36=0. 00000E+00

C
 I121

E37=0.160605E+05
 E38=0.913901E-32
 E39=0.962472E+03
 E310=0.203602E+02
 GO TO 50

C
 C
 1122

ANGS=0 ANGI=90 ANG=-10 ANGO=60

F11=0.790346E+04
 F12=-.196704E+01
 F13=0.301838E-07
 F14=-.142808E+03
 F15=0.291412E-01
 F16=-.117578E-24
 F17=0.705603E+02
 F18=-.200938E-24
 F19=0.634065E+01
 F110=-.262536E+03
 F21=-.563134E+02
 F22=0.119556E-01
 F23=0.987899E-08
 F24=0.130813E+02
 F25=0.340290E+00
 F26=-.470838E-26
 F27=0.114722E+04
 F28=0.148104E-25
 F29=0.534212E+02
 F310=0.129020E+01
 F31=-.122608E+04
 F32=0.260306E+00
 F33=0.214697E-06
 F34=0.286723E+03
 F35=0.740904E+01
 F36=-.103164E-24
 F37=0.249778E+05
 F38=0.318815E-24
 F39=0.116312E+04
 F310=0.280912E+02
 GO TO 50

C
 C
 1211

ANGS=-30 ANGI=150 ANG=-30 ANGO=60

F11=0.178657E+04
 F12=-.998658E-01
 F13=0.248111E-08
 F14=0.756883E+03
 F15=0.589541E+00
 F16=0.000000E+00
 F17=0.114030E+04

OPT02890
 OPT02900
 OPT02910
 OPT02920
 OPT02930
 OPT02940
 OPT02950
 OPT02960
 OPT02970
 OPT02980
 OPT02990
 OPT03000
 OPT03010
 OPT03020
 OPT03030
 OPT03040
 OPT03050
 OPT03060
 OPT03070
 OPT03080
 OPT03090
 OPT03100
 OPT03110
 OPT03120
 OPT03130
 OPT03140
 OPT03150
 OPT03160
 OPT03170
 OPT03180
 OPT03190
 OPT03200
 OPT03210
 OPT03220
 OPT03230
 OPT03240
 OPT03250
 OPT03260
 OPT03270
 OPT03280
 OPT03290
 OPT03300
 OPT03310
 OPT03320
 OPT03330
 OPT03340
 OPT03350
 OPT03360

OPT03370
OPT03380
OPT03390
OPT03400
OPT03410
OPT03420
OPT03430
OPT03440
OPT03450
OPT03460
OPT03470
OPT03480
OPT03490
OPT03500
OPT03510
OPT03520
OPT03530
OPT03540
OPT03550
OPT03560
OPT03570
OPT03580
OPT03590
OPT03600
OPT03610
OPT03620
OPT03630
OPT03640
OPT03650
OPT03660
OPT03670
OPT03680
OPT03690
OPT03700
OPT03710
OPT03720
OPT03730
OPT03740
OPT03750
OPT03760
OPT03770
OPT03780
OPT03790
OPT03800
OPT03810
OPT03820
OPT03830
OPT03840

E18=0. 236869E-24
E19=0. 936273E+02
E20=0. 104871E+04
E21=0. 194154E+00
E22=0. 990552E-08
E23=0. 843671E+04
E24=0. 310764E+01
E25=0. 000000E+00
E26=0. 439299E+04
E27=0. 119553E-24
E28=0. 195943E+03
E29=0. 708747E+04
E30=0. 167420E+00
E31=0. 109366E-07
E32=0. 884347E+04
E33=0. 414295E+01
E34=0. 000000E+00
E35=0. 646119E+04
E36=0. 623306E-24
E37=0. 659744E+03
E38=0. 659744E+03
E39=0. 659744E+03
GO TO 50

C
1221

ANGM=-10 ANGO=60

ANGS=-30 ANGI=150
E11=0. 641881E+04
E12=0. 154288E+01
E13=0. 611579E-06
E14=0. 822035E+03
E15=0. 654956E+00
E16=0. 225410E+04
E17=0. 125410E+04
E18=0. 571492E-14
E19=0. 978107E+02
E20=0. 211747E+03
E21=0. 386867E+04
E22=0. 264005E+01
E23=0. 210582E-05
E24=0. 112568E+05
E25=0. 284393E+01
E26=0. 540771E+03
E27=0. 348582E+04
E28=0. 136893E-13
E29=0. 465491E+03
E30=0. 379750E+03
E31=0. 128335E+05
E32=0. 147761E+01
E33=0. 331809E-05
E34=0. 870688E+04
E35=0. 451243E+01

F36=-. 169267E+04
F37=0. 690758E+04
F38=0. 428491E-13
F39=0. 713575E+03
F310=-. 186004E+03
GO TO 50

C
C
1131

ANGS=0 ANGI=120 ANGM=-20 ANGO=60
F11=0. 811671E+04
F12=-. 196614E+01
F13=-. 333818E-07
F14=0. 188933E+04
F15=0. 483956E-01
F16=0. 00000E+00
F17=-. 139207E+04
F18=0. 140756E-23
F19=0. 108259E+02
F110=-. 262390E+03
F21=-. 633443E+03
F22=0. 143016E+00
F23=-. 376307E-08
F24=0. 396744E+04
F25=0. 231410E+01
F26=0. 00000E+00
F27=0. 595382E+04
F28=0. 129334E-23
F29=0. 381170E+03
F310=0. 157266E+02
F31=-. 158742E+04
F32=0. 358846E+00
F33=-. 974890E-08
F34=0. 997180E+04
F35=0. 580637E+01
F36=0. 00000E+00
F37=0. 149255E+05
F38=0. 324027E-23
F39=0. 956405E+03
F310=0. 394602E+02
GO TO 50

C
C
1132

ANGS=0 ANGI=150 ANGM=-20 ANGO=60
F11=0. 759289E+04
F12=-. 195657E+01
F13=0. 870930E-08
F14=-. 874970E+03
F15=0. 965528E-01
F16=-. 807894E-23
F17=0. 867856E+03

OPT03850
OPT03860
OPT03870
OPT03880
OPT03890
OPT03900
OPT03910
OPT03920
OPT03930
OPT03940
OPT03950
OPT03960
OPT03970
OPT03980
OPT03990
OPT04000
OPT04010
OPT04020
OPT04030
OPT04040
OPT04050
OPT04060
OPT04070
OPT04080
OPT04090
OPT04100
OPT04110
OPT04120
OPT04130
OPT04140
OPT04150
OPT04160
OPT04170
OPT04180
OPT04190
OPT04200
OPT04210
OPT04220
OPT04230
OPT04240
OPT04250
OPT04260
OPT04270
OPT04280
OPT04290
OPT04300
OPT04310
OPT04320

E18=-. 131746E-24
 E19=0. 171856E+02
 E110=-. 261498E+03
 E21=-. 331499E+04
 E22=0. 472346E+00
 E23=0. 633018E-07
 E24=0. 348746E+04
 E25=0. 317480E+01
 E26=-. 549204E-24
 E27=0. 967072E+04
 E28=0. 226133E-23
 E29=0. 521581E+03
 E31=0. 609826E+02
 E32=-. 159741E+04
 E33=0. 682238E-01
 E34=0. 844020E-07
 E35=0. 497586E+04
 E36=-. 439744E+01
 E37=0. 181799E-23
 E38=0. 131649E+05
 E39=0. 309438E-23
 E310=-. 722932E+03
 CO TO 50

C

I141

ANG=0 ANCI=150 ANCM=-30 ANGO=60
 E11=0. 790298E+04
 E12=-. 196635E+01
 E13=0. 226082E-08
 E14=0. 696921E+02
 E15=0. 446845E-01
 E16=-. 330942E-04
 E17=0. 364668E+02
 E18=0. 205154E-20
 E19=0. 996732E+01
 E110=-. 262424E+03
 E21=-. 821164E+03
 E22=0. 181858E+00
 E23=-. 929652E-08
 E24=0. 915014E+04
 E25=0. 320679E+01
 E26=0. 104216E+04
 E27=0. 467566E+04
 E28=-. 623528E-13
 E29=0. 525775E+03
 E31=0. 199699E+02
 E32=-. 117923E+04
 E33=0. 248020E+00

OPT04330
 OPT04340
 OPT04350
 OPT04360
 OPT04370
 OPT04380
 OPT04390
 OPT04400
 OPT04410
 OPT04420
 OPT04430
 OPT04440
 OPT04450
 OPT04460
 OPT04470
 OPT04480
 OPT04490
 OPT04500
 OPT04510
 OPT04520
 OPT04530
 OPT04540
 OPT04550
 OPT04560
 OPT04570
 OPT04580
 OPT04590
 OPT04600
 OPT04610
 OPT04620
 OPT04630
 OPT04640
 OPT04650
 OPT04660
 OPT04670
 OPT04680
 OPT04690
 OPT04700
 OPT04710
 OPT04720
 OPT04730
 OPT04740
 OPT04750
 OPT04760
 OPT04770
 OPT04780
 OPT04790
 OPT04800


```

C C C
IF (TEST.EQ.1) R=PI
CALCULATE CONTROL INPUTS U1, '2 AND U3
U1=-(F11*X1(K)+F12*X2(K)+F13*(X3(K)-R)+F14*X4(K)+F15*X5(K)
2+F16*X6(K)+F17*X7(K)+F18*X8(K)+F19*X10(K)+F110*X11(K))
U2=-(F21*X1(K)+F22*X2(K)+F23*(X3(K)-R)+F24*X4(K)+F25*X5(K)
2+F26*X6(K)+F27*X7(K)+F28*X8(K)+F29*X10(K)+F210*X11(K))
U3=-(F31*X1(K)+F32*X2(K)+F33*(X3(K)-R)+F34*X4(K)+F35*X5(K)
2+F36*X6(K)+F37*X7(K)+F38*X8(K)+F39*X10(K)+F310*X11(K))

C C C C C
CALCULATE THE K+1 VALUE OF EACH VARIABLE
*****
X1(K+1)=X1(K)+T*O.0678345*U1
X2(K+1)=X2(K)+T*GAIN*(-CS*X1(K)+CI*SS*X4(K)-SI*CM*SS*X7(K)-
2Z*SO*SS*P)
X3(K+1)=X3(K)+T*(X1(K)-SM*X7(K)+CM*SO*P)
X4(K+1)=X4(K)+T*1/JM*U2
X5(K+1)=X5(K)+T*GAIN*(-CI*CS*X4(K)+CS*SI*CM*X7(K)-
2SS*X1(K)+Z*SO*CS*P)
X6(K+1)=X6(K)+T*(X4(K)-CO*P)
X7(K+1)=X7(K)+T*1/JO*U3-SM/JO*U1
X8(K+1)=X8(K)+T*(-CI*CM*X7(K)-SI*X4(K)-SO*CI*SM*P)
X9(K+1)=X9(K)+T*X7(K)
X10(K+1)=X10(K)+T*X5(K)
X11(K+1)=X11(K)+T*X2(K)

C C C C C 10 C C C C C 998
IF (K.EQ.2800) GO TO 777
CONTINUE

TTT=T*K
CALL FRTCMQ('CLRSCRN ')
PRINT *,',',
PRINT *,',',
PRINT *,',',
PRINT *,',',
PRINT *,',',
OPTIMAL FEEDBACK GAINS HAVE NOT BEEN COMPUTED,
FOR THE CURRENT GIMBAL ANGLES. NULLING SIN(AI),

```

OPT05770
 OPT05780
 OPT05790
 OPT05800
 OPT05810
 OPT05820
 OPT05830
 OPT05840
 OPT05850
 OPT05860
 OPT05870
 OPT05880
 OPT05890
 OPT05900
 OPT05910
 OPT05920
 OPT05930
 OPT05940
 OPT05950
 OPT05960
 OPT05970
 OPT05980
 OPT05990
 OPT06000
 OPT06010
 OPT06020
 OPT06030
 OPT06040
 OPT06050
 OPT06060
 OPT06070
 OPT06080
 OPT06090
 OPT06100
 OPT06110
 OPT06120
 OPT06130
 OPT06140
 OPT06150
 OPT06160
 OPT06170
 OPT06180
 OPT06190
 OPT06200
 OPT06210
 OPT06220
 OPT06230
 OPT06240

```

PRINT *, , ANG= , ANG
PRINT *, , ANGI= , ANGI
PRINT *, , ANGM= , ANGM
PRINT *, , ANGO= , ANGO
PRINT *, ,
PRINT *, ,
PRINT *, , K= , K
PRINT *, , T= , TT
PRINT *, , P= , P
GO TO 777

TTT=T*K
CALL FRTCMS( 'CLRSCRN ' )
PRINT *, ,
PRINT *, ,
PRINT *, ,
PRINT *, ,
PRINT *, ,
PRINT *, , ANG= , ANG
PRINT *, , ANGI= , ANGI
PRINT *, , ANGM= , ANGM
PRINT *, , ANGO= , ANGO
PRINT *, ,
PRINT *, , K= , K
PRINT *, , T= , TT
PRINT *, , P= , P
GO TO 777

DO 80 I=1,K,25
TT=T*I
WRITE GYRO ERRORS TO ERR DATA FILE

UGSGF=X2{ I }
VGS GF=X5{ I }

WRITE GIMBAL ANGLES TO ANG DATA FILE

ANGI=X3( I ) *180/PI
ANGM=X6( I ) *180/PI
ANGS=X8( I ) *180/PI
ANGO=X9( I ) *180/PI
WRITE ( 7,30) TT,UGSGF,VGS GF,ANGI,ANGM
FORMAT( 5E14.6)
WRITE ( 8,40) TT,ANGI,ANGM,ANGS,ANGO
FORMAT( 5E14.6)
CONTINUE
30
40
80
C

```

OPT06730
OPT06740
OPT06750

STOP
END

C

APPENDIX D TABULATED DATA

TIME (SEC)	UCSCF	VGSCF	INNER ANGLE	MIDDLE ANGLE
0.333333E-03	0.000000E+00	0.000000E+00	0.900000E+02	0.000000E+00
0.866666E-02	0.277583E-04	0.145522E-01	0.900143E+02	-0.846295E-02
0.170000E-01	0.103715E-02	-0.133000E+00	0.900559E+02	-0.332002E-01
0.253333E-01	0.662004E-02	-0.385341E+00	0.901224E+02	-0.742088E-01
0.336666E-01	0.219164E-01	-0.762853E+00	0.902211E+02	-0.131484E+00
0.419999E-01	0.524355E-01	-0.1266719E+01	0.903448E+02	-0.205019E+00
0.508333E-01	0.181147E+00	-0.189803E+01	0.904958E+02	-0.294804E+00
0.586666E-01	0.289998E+00	-0.265487E+01	0.906741E+02	-0.400826E+00
0.669999E-01	0.435436E+00	-0.353736E+01	0.908799E+02	-0.523072E+00
0.753333E-01	0.622578E+00	-0.454502E+01	0.911130E+02	-0.661523E+00
0.836666E-01	0.856513E+00	-0.567730E+01	0.913735E+02	-0.816158E+00
0.919999E+00	0.114231E+01	-0.693336E+01	0.916613E+02	-0.986950E+00
0.108667E+00	0.148502E+01	-0.831394E+01	0.919766E+02	-0.117388E+01
0.117000E+00	0.188966E+01	-0.981594E+01	0.923193E+02	-0.137688E+01
0.125333E+00	0.236123E+01	-0.114406E+02	0.926899E+02	-0.159594E+01
0.133667E+00	0.290470E+01	-0.131867E+02	0.930512E+02	-0.183100E+01
0.142000E+00	0.352500E+01	-0.150534E+02	0.933964E+02	-0.208201E+01
0.150866E+00	0.420202E+01	-0.170402E+02	0.939646E+02	-0.234891E+01
0.158666E+00	0.507115E+01	-0.191464E+02	0.944444E+02	-0.263162E+01
0.167000E+00	0.589571E+01	-0.213711E+02	0.949527E+02	-0.293006E+01
0.175333E+00	0.687201E+01	-0.237139E+02	0.954882E+02	-0.324414E+01
0.183666E+00	0.794933E+01	-0.261741E+02	0.960516E+02	-0.357375E+01
0.192000E+00	0.913224E+01	-0.287511E+02	0.966422E+02	-0.391879E+01
0.200866E+00	0.104209E+02	-0.314444E+02	0.972620E+02	-0.427913E+01
0.209666E+00	0.116226E+02	-0.340490E+02	0.979065E+02	-0.465295E+01
0.217000E+00	0.138379E+02	-0.368033E+02	0.985557E+02	-0.502813E+01
0.225333E+00	0.166588E+02	-0.404485E+02	0.992014E+02	-0.540227E+01
0.233666E+00	0.204655E+02	-0.449793E+02	0.998553E+02	-0.577522E+01
0.242000E+00	0.245961E+02	-0.500799E+02	0.998553E+02	-0.614706E+01
0.250866E+00	0.292444E+02	-0.55961E+02	0.101155E+03	-0.651756E+01
0.259666E+00	0.341474E+02	-0.628444E+02	0.101813E+03	-0.688676E+01
0.267000E+00	0.390133E+02	-0.701181E+02	0.102467E+03	-0.7225461E+01
0.275333E+00	0.438333E+02	-0.770531E+02	0.103778E+03	-0.762105E+01
0.283666E+00	0.483933E+02	-0.840015E+02	0.104436E+03	-0.798606E+01
0.292000E+00	0.529299E+02	-0.914141E+02	0.105095E+03	-0.834959E+01
0.300866E+00	0.572488E+02	-0.997000E+02	0.105755E+03	-0.871125E+01
0.309666E+00	0.6159717E+02	-0.390406E+03	0.106415E+03	-0.906673E+01
0.317000E+00	0.6597174E+02	-0.399967E+03	0.107077E+03	-0.942558E+01
0.325333E+00	0.703000E+02	-0.180456E+03	0.107741E+03	-0.977518E+01
0.333666E+00	0.746991E+02	-0.184598E+03	0.108401E+03	-0.101213E+02
0.342000E+00	0.792207E+02	-0.188565E+03	0.109071E+03	-0.104636E+02
0.350866E+00	0.838572E+02	-0.180980E+03	0.109737E+03	-0.108017E+02
0.359666E+00	0.885717E+02	-0.176057E+03	0.110405E+03	-0.111359E+02
0.367000E+00	0.93377E+02	-0.170973E+03	0.111074E+03	-0.114662E+02
0.375333E+00	0.204042E+03	-0.166263E+03	0.111745E+03	-0.117927E+02
0.383666E+00		-0.161582E+03	0.112417E+03	-0.121154E+02
0.392000E+00				-0.124343E+02

LIST OF REFERENCES

1. C. S. Draper Laboratory Report CSDL-P-1858, A Discrete Time Cost-Optimal Regulator for the All-Attitude Gimbal Assembly, by G. Lauro, February 1984
2. Martinage, L., Four Gimbal IMU Model, C. S. Draper Laboratory memorandum 20E:73:82.
3. C. S. Draper Laboratory Report, Electronics Design Review, 18 December 1985.
4. Kwakernaak, H. and Sivan, R., Linear Optimal Control Systems, John Wiley & Sons, Inc., 1972.

INITIAL DISTRIBUTION LIST

	No.	Copies
1. Defense Technical Information Center Cameron Station Alexandria, Virginia 22304-6145		2
2. Superintendent Attn: Library, Code 0142 Naval Postgraduate School Monterey, California 93943-5000		2
3. Superintendent, Code 67Co Attn: Professor D.J. Collins, Dept. of Aeronautics Naval Postgraduate School Monterey, California 93943-5000		2
4. Charles Stark Draper Laboratory Education Office Mail Stop 02 555 Technology Square Cambridge, Massachusetts 02139		2
5. Lieutenant David L. Krueger, U.S. Navy 12619 Meadowood Drive Silver Spring, Maryland 20904		6

END
DITIC

7-86